ACADÉMIE DES SCIENCES
INSTITUT DE FRANCE

Comptes Rendus

Physique

Pierre Darriulat, Do Thi Hoai, Pham Thi Tuyet Nhung, Pham Ngoc Diep,
Nguyen Bich Ngoc, Tran Thi Thai and Pham Tuan Anh

On the nascent wind of oxygen-rich AGB stars: scrutiny of a sample of nearby stars

CENTRE MERSENNE

ACADÉMIE
DES SCIENCES
INSTITUT DE FRANCE

Review article / *Article de synthèse*

On the nascent wind of oxygen-rich AGB stars: scrutiny of a sample of nearby stars

Genèse du vent des étoiles riches en oxygène de la branche AGB : examen d'un échantillon d'étoiles proches

Pierre Darriulat [©], [*], [a]**, Do Thi Hoai** [©], [a]**, Pham Thi Tuyet Nhung** [©], [a]**, Pham Ngoc Diep** [©], [a]**, Nguyen Bich Ngoc** [©], [a]**, Tran Thi Thai** [©], [a] **and Pham Tuan Anh** [©], [a]

[a] Department of Astrophysics, Vietnam National Space Center, Vietnam Academy of Science and Technology, 18, Hoang Quoc Viet, Nghia Do, Cau Giay, Ha Noi, Vietnam

E-mails: darriulat@vnsc.org.vn (P. Darriulat), dthoai@vnsc.org.vn (D. T. Hoai), pttnhung@vnsc.org.vn (P. T. Nhung), pndiep@vnsc.org.vn (P. N. Diep), ntbngoc@vnsc.org.vn (N. B. Ngoc), ttthai@vnsc.org.vn (T. T. Thai), ptanh@vnsc.org.vn (P. T. Anh)

Abstract. The commonly accepted mechanism governing the formation of the nascent wind in oxygen-rich AGB stars combines an initial boost above the photosphere, given by shock waves resulting from stellar pulsations and convective cell partition, with a subsequent acceleration fuelled by the radiation pressure of the star on dust grains. We use six nearby stars, for which detailed studies of visible and infrared observations at the VLT and millimetre observations at ALMA are available, to assess the extent to which the validity of this picture is currently corroborated. We show that while providing a very useful guide to current research and having received general support and suffered no contradiction, it still requires many additional observations to be reliably validated. In particular, observations of the highest possible angular resolution at both millimetre and visible/infrared wavelengths, performed in conjunction with measurements of the light curve, are necessary to tell apart the respective roles played by convection and stellar pulsations. The observed concurrence of high variability near the photosphere with persistence over decades, or even centuries, of the global anisotropy displayed by the CSE needs to be understood. New observations of the close neighbourhood of the star are required to elucidate the mechanism that governs rotation, in particular in the cases of R Dor, L_2 Pup and EP Aqr. We argue that the presence of stellar or planetary companions does not seriously impact the formation of the nascent wind and only modifies its subsequent evolution.

Résumé. Le mécanisme couramment accepté comme présidant à la formation du vent des étoiles AGB riches en oxygène combine deux effets : un élan initial qui projette le gaz au-dessus de la photosphère, donné par des ondes de choc produites par pulsations stellaires et cellules de convection, suivi d'une accélération alimentée par la pression de radiation stellaire sur des grains de poussière. Nous examinons dans quelle mesure ce modèle est corroboré par les observations de six étoiles proches faites dans les domaines du visible/infrarouge par le VLT et dans le domaine millimétrique par ALMA. Nous montrons que bien que généralement corroboré, n'ayant souffert aucune contradiction et servant utilement de guide aux recherches actuelles, il a encore besoin de nombreuses observations complémentaires pour être validé de manière fiable. En particulier, afin de mieux préciser les rôles joués par pulsations stellaires et mouvements de convection, il faudra mesurer la courbe de lumière en même temps qu'on observera, avec la meilleure résolution angulaire possible, les émissions des domaines millimétrique et visible/infrarouge. Il faudra clarifier comment la grande variabilité révélée par les observations de la photosphère est compatible avec la persistance sur des

---

[*] Corresponding author.

décennies, voire des siècles, de l'anisotropie de l'enveloppe. De nouvelles observations du gaz proche de l'étoile seront nécessaires pour préciser le mécanisme présidant à sa rotation, en particulier pour R Dor, L$_2$ Pup et EP Aqr. Nous suggérons que la présence de compagnons stellaires ou planétaires n'a pratiquement pas d'impact sur la genèse du vent et ne fait que modifier son évolution ultérieure.

1. Introduction

1.1. *State-of-the-art*

Much progress has been made over the past decade in understanding the mechanisms at stake in the formation of the nascent wind of oxygen-rich AGB stars. The most salient features have recently been described, in particular by B. Freytag, S. Höfner, S. Liljegren and H. Olofsson in a series of recent papers, in terms that we summarise below; we refer the reader to these articles [1–4] for a list of relevant references. For simplicity, in the remainder of this article, we refer to such description as "the current model".

In contrast to carbon-rich, oxygen-rich AGB stars have a dusty envelope that is more transparent in the visible and near-infrared, giving a better view of the innermost dust-forming atmospheric layers. Their study supports a scenario where the radiation pressure, which triggers the outflows, is caused by photon scattering on highly transparent iron-free dust grains, which condense at shorter distances than iron-bearing silicate grains. As long as they are of a size comparable to the radiation wavelength, ~0.1–1.0 µm, they uphold sufficient radiation pressure. Studies of dust formation [5–9] suggest that the condensation of corundum (Al_2O_3), forming a thin dust layer close to the stellar photosphere, precedes the formation of silicate dust, the condensation of silicate mantles on top of corundum cores speeding up grain growth to the critical size.

Recent high-resolution imaging of nearby AGB stars at visible and infrared wavelengths has revealed complex, non-spherical distributions of gas and dust in the close circumstellar environment, with changes in morphology and grain sizes occurring over the course of weeks or months. Such inhomogeneous distribution of atmospheric gas emerges naturally in 3-D hydrodynamical models, as a consequence of large-scale convective flows below the photosphere and the resulting network of atmospheric shock waves, the dynamical patterns in the gas being imprinted on the dust in the close stellar environment. Global AGB star models [10] are characterised by giant convection cells, which can span over a steradian, and have a lifetime of many years. The photospheric layers have a complex, variable appearance due to smaller, shorter-lived cells, which form close to the surface of the convection zone. In addition to the convective flows, radial pulsations occur with typical periods at year scale. These dynamical processes generate waves of various frequencies and spatial scales, which quickly develop into shock waves as they propagate outward through the atmosphere with its steeply declining density. The shocks give rise to ballistic gas motions, which typically peak around 2 stellar radii. As the shock waves interact and merge, they produce large-scale regions of enhanced densities in their wakes.

As remarked by Höfner and Freytag [3], the basic formation mechanism of the dust cloud precedes wind acceleration. Its study is therefore a necessary preliminary to the understanding of the mass-loss mechanism; in this context, the acceleration of the wind, its possible subsequent interaction with planetary or stellar companions, and more generally the evolution towards the

planetary nebula phase, appear as complications that can be ignored. This early phase of formation of the nascent wind appears instead as fundamental and its study deserves being dedicated major effort on both theoretical and observational fronts. Recently, two main approaches have been pursued towards this aim: observations in the visible and infrared, essentially using the VLT, and millimetre observations, essentially using ALMA.

The former, using the VLT in single-dish or interferometer mode, take advantage of the high performance of instruments such as SPHERE-ZIMPOL. Particularly remarkable are observations of π^1 Gruis [11] using PIONIER, which show evidence for the presence of large granulation cells on the stellar surface. In this context, using the same instrument, one must recall the observation of granulation on the surface of Betelgeuse [12] and its confirmation from spectro-polarimeter observations [13] using NARVAL at Pic du Midi; the latter give evidence for slow evolution of the granule pattern on a 2 to 3 years timescale, accompanied by a much faster variability with small amplitude variations of a week-to-month time scale. NARVAL observations have also given evidence for asymmetric shocks in χ Cygni, induced by the interplay between pulsation and convection, suggesting the presence of a highly anisotropic and variable velocity field near the surface of the star [14].

In general, evidence for clumpy dust clouds near the star has been obtained from the detection of scattered light and multi-epoch observations have shown changes in morphology on month time scales. They have provided evaluations of the dust grain size consistent with the picture described above.

Millimetre observations have concentrated on three fronts: (1) study of the continuum emission of the stellar disc and surrounding hot dust, giving occasional evidence for hot spots and variability; (2) measurements of the radial dependence of the abundance of molecular species giving evidence, in particular, for the early formation of aluminium-rich dust grains; (3) measurements of the morpho-kinematics of the inner CSE layer using the emission of molecular lines.

1.2. *Six selected stars*

We have selected a sample of six well-studied oxygen-rich AGB stars to illustrate the most salient features displayed by the morpho-kinematics of their inner CSE layers. All stars in the sample are oxygen-rich nearby stars, with spectral type M and within 100 pc or so from the Sun. Their masses cover between ~0.7 and ~2 solar masses. Most are long period variables with periods at year scale [15], with the exception of EP Aqr and L_2 Pup, which have periods of only 110 and 141 days, respectively. The period-luminosity relation shows that EP Aqr pulsates on the first overtone while all others pulsate in the fundamental mode. They are shared between Mira and semi-regular types, but the separation between the two classes is sometimes unclear (e.g. W Hya). None shows a clear technetium signal in its spectrum [16] but *o* Cet [17, 18] and L_2 Pup [19] may display some. All have low mass-loss rates, not exceeding ~2×10^{-7} solar masses per year. *o* Cet has a clearly identified companion of mass 0.7 solar masses with a separation of ~80 au and displays features characteristic of symbiotic systems. Kervella *et al.* [20] have claimed the presence of a planetary companion distant by only 2 au from the centre of L_2 Pup but this needs to be confirmed. Important parameters are listed in Table A1 of the Appendix A, together with references of relevance to the present article. Table A2 lists molecular lines considered in the present review and observed with high angular resolution, together with relevant parameters and associated beam sizes.

At first glance, each of the oxygen-rich AGB stars that have been studied in some detail displays properties of its own making it appear as somewhat singular: unveiling common properties that can be considered as characteristic of the whole family is therefore very challenging. The aim of the present article is to make a step in this direction.

2. The stellar disc and its immediate environment

ALMA observations of continuum emission have provided images of the stellar disc and of its immediate environment at millimetre wavelengths, often displaying variability and hot spots interpreted as the effect of shocks induced by pulsations and convective cell partition.

The disc of *o* Cet has been shown to have a 10% to 20% ellipticity in early measurements using JVLA [21, 22], ISI [23] and IOTA [24], but was found circular later on [25, 26]. Kamínski *et al.* [27], also using APEX and Herschel observations, have given evidence for strong inhomogeneity (hot spot) and irregular variability in the emission of AlO molecules. Spectro-polarimeter observations using NARVAL at Pic du Midi [28] have given evidence for shock-induced polarised hydrogen emission lines, suggesting their association with convective cells.

Strong hot spots have been observed on W Hya, with lifetimes at the scale of weeks [26, 29] and on R Dor [26], correlated with dust structures observed in the visible. However, no hot spot has been directly observed on R Leo and EP Aqr; in the former case, Vlemmings *et al.* [26] have given evidence for a radial asymmetric expansion with mean velocity of 10.6 ± 1.4 km·s^{-1} within 1–2 stellar radii; in the latter case, Homan *et al.* [30] have given evidence for a 20% flux density increase between 2016 and 2019, suggesting variability and sporadic contributions on scales larger than the stellar disc.

Observations using the VLT, at optical and infrared wavelengths, have given evidence for a dusty layer surrounding the photosphere, commonly displaying both inhomogeneity and variability. In particular SPHERE/ZIMPOL polarisation measurements are available for L$_2$ Pup [31], for *o* Cet [32], for W Hya [9,33,34], for R Dor [35] and for EP Aqr [30]. The degree of linear polarisation usually reaches high values, well in excess of 10%, except for *o* Cet, where it does not exceed 4%, dust being confined at the border of a dense gas reservoir, within 100–200 mas (10–20 au) from the centre of the star. In the case of W Hya, together with observations using NACO [36], AMBER/VLTI [9, 33, 37] and MIDI/VLTI [38], evidence is obtained for a clumpy and dusty layer, displaying significant variability at short time scale. In the case of R Dor, Khouri *et al.* [35] find evidence for variability and asymmetry, with outflwing dust of steeply decreasing radial density and Ohnaka *et al.* [39], using VLTI/AMBER, find evidence for sudden outward acceleration to 7–15 km·s^{-1} at radial distances between 1.5 and 1.8 stellar radii. In the case of EP Aqr [30], the linearly polarised flux map suggests the presence of a torus of dust with an axis close to the known axi-symmetry axis of the CSE. Finally, the close neighbourhood of R Leo has been observed in the near-infrared [40] using VLTI/VINCI, giving evidence for significant deviation from a uniform disc profile, and in the mid-infrared by Paladini *et al.* [41] using VLTI/MIDI, showing unusually large spectral shape variations and giving evidence for brightness inhomogeneity appearing already in the dust-forming region.

The case of L$_2$ Pup is outstanding. Its light curve [42–44] has been undergoing a major dimming episode in ~1994. NACO observations together with VINCI observations [45], and together with AMBER/VLTI observations [46, 47], have revealed a dust disc, oriented east–west and inclined by ~82° with respect to the plane of the sky, with approximate projected size of 180×50 mas^2 (11.5×3.2 au^2). Ohnaka *et al.* [47] and Bedding *et al.* [43] assume that dust clouds were ejected at the end of the past century, causing the formation of the circumstellar disc. Others assume instead that it existed before the dimming event and, in 1994, simply started obscuring significantly the star. ALMA observations of continuum emission [20] show a slight E–W elongation caused by hot dust in the circumstellar disc. Finally, using SPHERE ZIMPOL observations, Kervella *et al.* [31] have claimed the presence of a companion at ~2.1 au west of the star, but the NACO images and the VINCI interferometer observations do not see trace of it.

One generally finds evidence for the presence of large transparent dust grains very close to the photosphere, in agreement with the seminal paper of Norris *et al.* [36] where VLT/NACO
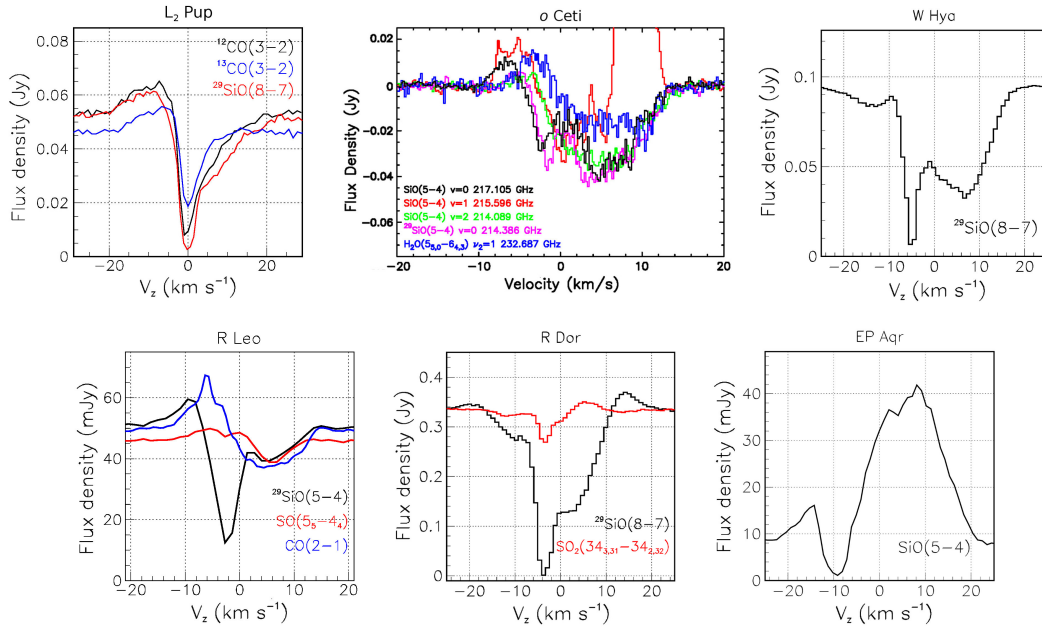
Figure 1. Doppler velocity spectra observed over the stellar disc. From left to right and up-down: L$_2$ Pup [49], ^{12,13}CO(3–2) and ^{29}SiO(8–7), 27 mas (1.7 au) FWHM beam; *o* Cet [25], ^{28,29}SiO(5–4), 32 mas (3.2 au) FWHM beam; W Hya [50], ^{29}SiO(8–7), 47 mas (4.9 au) FWHM beam; R Leo [51], CO(2–1), ^{29}SiO(5–4) and SO(5$_5$–4$_4$), 42 mas (4.8 au) FWHM beam; R Dor [52], ^{29}SiO(8–7) and SO$_2$(34$_{3,31}$–34$_{2,32}$), 38 mas (2.2 au) FWHM beam; EP Aqr [53], SiO(5–4), 32 mas (3.8 au) FWHM beam.

observations of W Hya, R Dor and R Leo were reported; in particular, dust grains surrounding W Hya, mostly aluminium composites [7], are found to have sizes ranging between 0.1 and 0.5 μm.

Finally, Khouri *et al.* [48] have detected emission from highly excited OH lines ($E_{\text{up}} > 4800$ K) within a very few au from the centres of W Hya and R Dor, giving evidence for the presence of strong shock fronts.

3. Molecular line spectra: absorption over the stellar disc

High angular resolution millimetre observations have revealed strong absorption of molecular line emission over the stellar disc. Wong *et al.* [25] were first to give a detailed description in the case of *o* Cet. Such absorption is particularly large for SiO lines and is often found to extend beyond the stellar disc in the form of self-absorption. Absorption spectra observed over the stellar disc provide important information on the morpho-kinematics of the inner layer, in particular giving evidence for in-falling gas. They probe the central line of sight independently from maximal recoverable scale constraints and the explored radial range depends only on the radial distribution of the abundance of the molecule being studied and on the range of temperatures associated with the particular transition.

Figure 1 displays such spectra measured on the six stars studied in the present article. In all cases, and in the whole article, they are referred to the systemic star velocity. They show an absorption peak on the blue-shifted side, at terminal velocity, revealing the opacity of the CSE

layer farther away from the star. In the case of L_2 Pup, where this layer is dominated by an edge-on rotating gravitationally bound disc, the absorption peak is centred at the origin. In the case of *o* Cet, where SiO molecules are confined within ~0.5 arcsec (50 au) from the centre of the star, the terminal velocity is probed by the emission of CO lines but not by that of SiO lines.

With the exception of EP Aqr, all show absorption on the red-shifted side, accounting for a significant fraction of the continuum emission, usually interpreted as evidence for in-falling gas. The dominance of red-shifted absorption is qualitatively consistent with the remark that the spectra illustrated in Figure 1 are generally measured near the minimum of the light curve: the phases for *o* Cet, W Hya, R Leo and R Dor are 0.45, 0.3, 0.5 and 0.5, respectively. L_2 Pup is outstanding: the spectra were measured on November 5, 2015, approximately one month after the expected maximum light, which, however, did not occur [20]: the magnitude stayed near minimum, regular oscillations resuming in early 2016 with smaller amplitude than in 2014.

Finally, there exists no measurement of the EP Aqr light curve, unfortunately preventing a reliable interpretation of the absence of red-shifted absorption. As the beam is usually larger than the stellar disc, some emission from gas located farther away from us than the star is leaking into the spectrum. In case of dominant infall, it is seen as blue-shifted, in case of dominant outflow, it is seen as red-shifted. In the present case, the ratio between the beam FWHM and the diameter of the stellar disc is 13.5/12 ~ 1.1, 16/21 ~ 0.8, 23.5/26 ~ 0.9, 21/21 ~ 1, 19/32 ~ 0.6 and 16/8 ~ 2 for L_2 Pup, *o* Cet, W Hya, R Leo, R Dor and EP Aqr, respectively. Its large value in the case of EP Aqr weakens the significance of the absence of red-shifted absorption. All spectra show evidence for significant wings of large velocities that are discussed in Section 5.

4. Outflowing gas

4.1. *Close to the star*

Gas escaping the central gravitationally bound reservoir does so in the form of outflows covering solid angles at steradian scale and having mean radial velocities of a few km·s^{-1}. This is a common feature observed in all six stars but taking different forms in each of them.

o Cet, R Leo and R Dor display particularly complex morpho-kinematics seen as patchy emission in the close neighbourhood of the stars. On *o* Cet (Figure 2), ALMA observations [54, 55] of SiO(5–4) and ^{12,13}CO(3–2) line emissions have given evidence for three ongoing CO outflows: one blowing south-east towards Mira B and two blowing north-east and south-west with Doppler velocities V_z ~ −3 km·s^{-1}. Moreover, evidence is also found for recent ejections of a north-eastern arc at V_z ~ +2 km·s^{-1} and a south-western outflow in the plane of the sky. A soft X-ray outburst was observed in 2003 [56] using CHANDRA/ACIS-S, probably caused by a magnetic flare followed by a large mass ejection.

R Leo has been studied [51] using ALMA observations of ^{29}SiO(5–4), CO(2–1), SO(5_5,4_4) and SO$_2$($22_{2,20}$–$22_{1,21}$) line emissions, giving evidence for three ongoing outflows covering broad solid angles in the south-eastern, south-western and north-western quadrants with low Doppler velocities at km·s^{-1} scale (Figure 3). The study of the relative abundance of different molecules in these outflows suggests that Local Thermal Equilibrium is violated close to the star, between ~2 and ~10 stellar radii, and is progressively restored when moving outward to ~30 stellar radii. In addition, like in *o* Cet, detached patches of emission are observed, the one closest to the star having Doppler velocity V_z = 2–3 km·s^{-1}, position angle ~260° and projected distance from the star between 1 and 2 arcsec.

In the case of R Dor (Figure 4), multiline ALMA observations [57] have shown that projected distances between ~20 and ~100 au host a radial wind with Doppler velocities reaching up
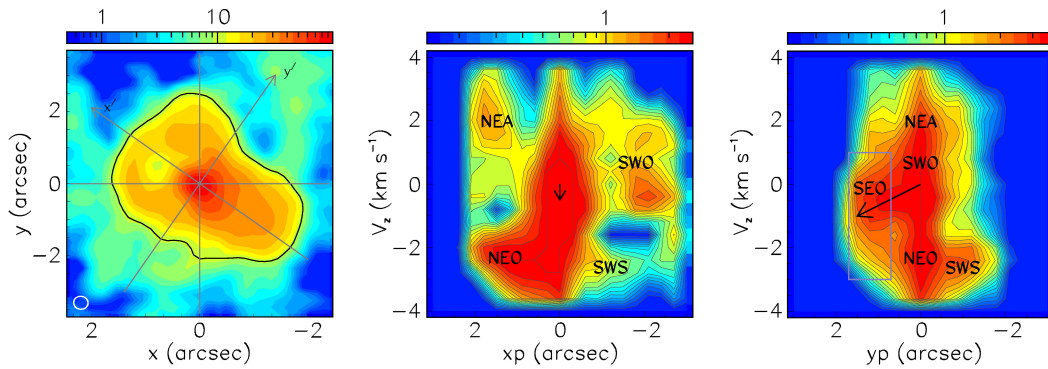
Figure 2. Outflows from *o* Cet [54]. Left: map of the $^{12}CO(3–2)$ intensity (Jy·km·s^{-1}·arcsec^{-2}) integrated over $|V_z| < 4$ km·s^{-1}. Middle and right: $^{13}CO(3–2)$ PV maps, V_z vs x' (middle) and V_z vs y' (right) defined in the left panel. The labels SWS, NEA, SWO and NEO stand for south-western stream, north-eastern arc, south-western outflow and north-eastern outflow, respectively; the arrow and the blue lines refer to the south-eastern outflow (SEO) dominated by the wind blowing from Mira A to Mira B. The colour scales are in units of Jy·arcsec^{-1}.
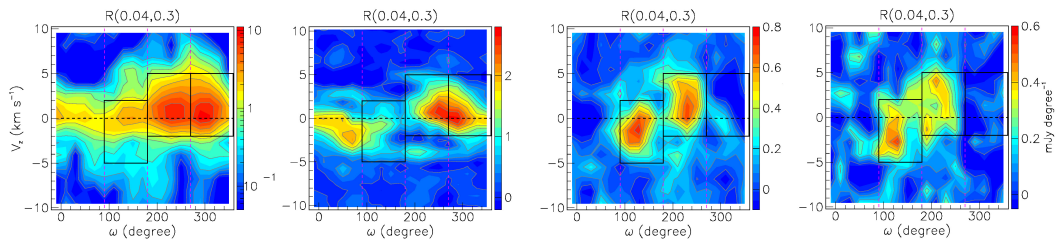

Figure 3. Outflows from R Leo [51]. PV maps, Doppler velocity V_z vs position angle ω, integrated over projected distances from the star $0.04 < R < 0.30$ arcsec (4.6 to 34.2 au). From left to right: SiO, CO, SO and SO$_2$ emissions. The black rectangles locate three regions of enhanced emission associated with different intervals of R.

to ~6 km·s^{-1}, characterised by strong inhomogeneity, both in angle and radially, as had been noted earlier by De Beck and Olofsson [58]. In particular, observations of the emission of the SO(6_5–5_4) line show that the presence of separate cores, of which seven have been identified and studied; at short distances from the star, the combined effect of expansion and rotation complicates the analysis of the morpho-kinematics. Particularly outstanding is a blue-shifted stream observed at ~140° position angle to extend radially from ~10 to ~30 au [52], which can be interpreted as a mass ejection that took place 5 to 10 years ago with a mean radial velocity of 15±5 km·s^{-1} but not as evidence for an evaporating planetary companion, as had been suggested earlier [6, 59, 60].

The cases of W Hya and L$_2$ Pup are different, with a single ongoing outflow identified in each case (Figure 5). W Hya has been shown [50], using ALMA observations of $^{12}CO(3–2)$ and $^{29}SiO(8–7)$ emissions, to host a recent mass ejection covering a broad cone with an axis making an angle of some 30° with the line of sight, and a blob of enhanced emission located some 0.2 arcsec (20 au) above the plane of the sky. Within the cone, and within radial distances confined to less than 25 au from the centre of the star, the number density is increased by an order of magnitude,
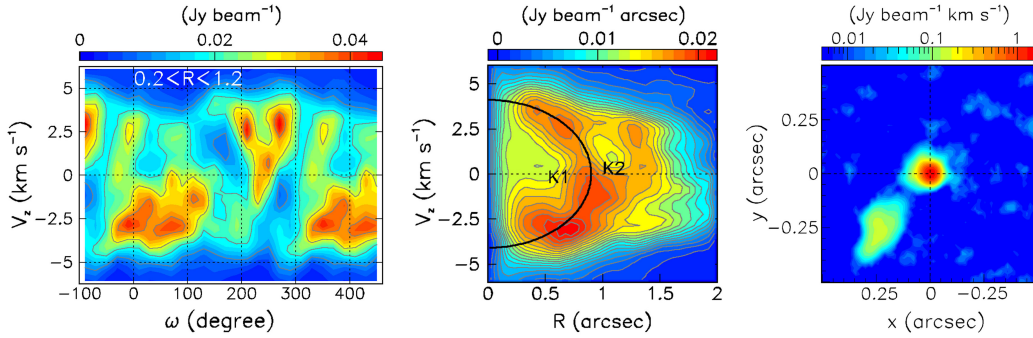
Figure 4. Outflows from R Dor, SO(6_5–5_4) emission [57]. Left: P-V map (Doppler velocity V_z vs position angle ω) integrated over projected distances from the star $0.2 < R < 1.2$ arcsec (11.8 to 71.8 au). Middle: *P–V* map of the product brightness × angular distance R in the V_z vs R plane, averaged over ω, showing toroidal cavity K_1 (and possibly K_2), giving evidence for a recent episode of enhanced mass loss. Right: the blue-shifted stream seen in ^{29}SiO(8–7) emission [52]. The intensity map is integrated over $-18.7 < V_z < -6.3$ km·s^{-1}.
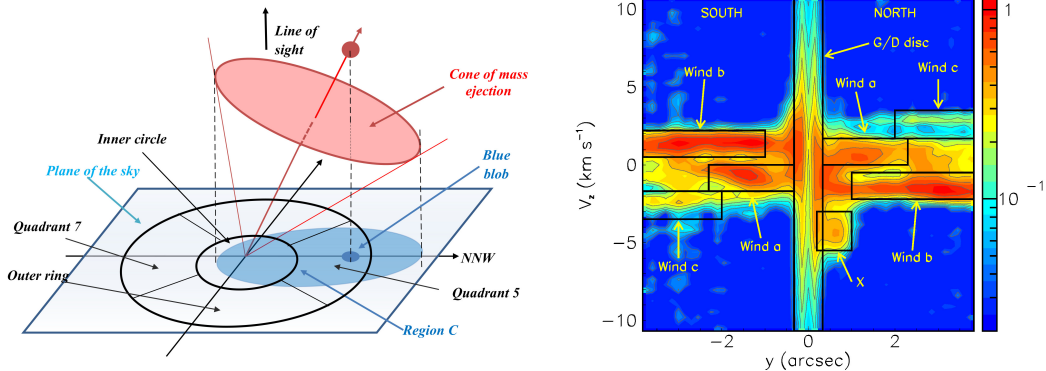

Figure 5. Outflows from W Hya (left, [50]) and L_2 Pup (right, [49]). Left: schematic geometry of the mass ejection from W Hya. Right: PV map of the ^{12}CO(2–1) emission of L_2 Pup in the V_z vs y plane integrated over the wedge $|\sin\omega| < 0.5$. The central gas-and-dust disc is indicated as G/D disc and the ongoing outflow mentioned in the text is indicated as X. The colour scale is in units of Jy·arcsec^{-1}.

with a SiO/CO ratio larger by at least a factor 2, and the effective line width is also about twice as large. The mean radial velocity inside the cone is 6–7 km·s^{-1}. The cone geometry matches the dust distribution observed using SPHERE/ZIMPOL at the VLT [33].

Close to the star, the CSE of L_2 Pup is dominated by a gas-and-dust disc in rotation, nearly edge-on. It may be slightly expanding at a rate of 0.8 ± 0.5 km·s^{-1}. It has been studied using ALMA observations of ^{29}SiO(8–7) emission [20], of ^{12,13}CO(3–2) emission [61] and ^{29}SiO(8–7), ^{12,13}CO(3–2) and ^{28}SiO(5–4) emissions [49]. An ongoing northern outflow with V_z between -5 and -3 km·s^{-1} is visible in ^{12}CO and ^{28}SiO emissions and probably associated with a feature seen in NACO infrared images [45]; it is the only candidate mass ejection that can be clearly identified [49].
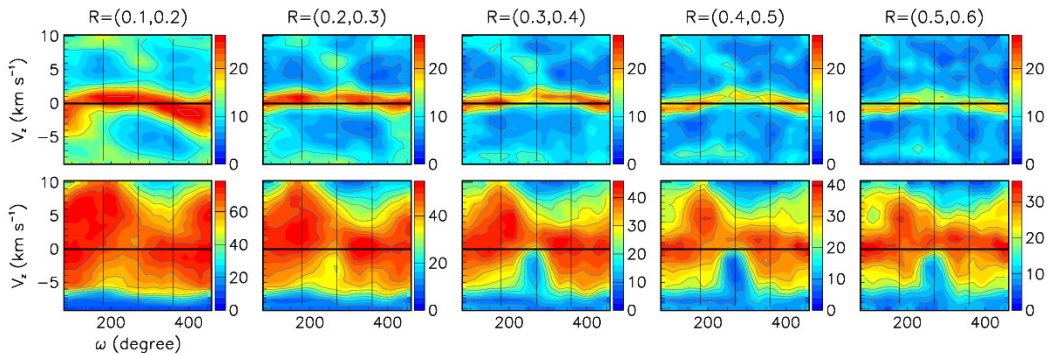
Figure 6. EP Aqr [53]. PV maps (Doppler velocity vs position angle) integrated over five successive intervals of angular distance as indicated on top of the panels in arcsec. In the upper row CO(2–1) emission is dominated by a disc, in the lower row SiO(5–4) emission is dominated by a pair of outflows.

The case of EP Aqr is outstanding (Figure 6). In addition to two broad outflows observed in SiO(5–4) line emission, of a similar nature as those observed in the other stars of the sample, a circumstellar disc in rotation, displaying emission dominated by CO lines, is observed to be formed very close to the photosphere. While Homan *et al.* [30, 62] have proposed an interpretation in terms of a white dwarf companion orbiting the star at an angular distance of ~400 mas (48 au), a recently published interpretation [53] relies on a different mechanism for the formation of the circumstellar disc and describes the observed morpho-kinematics of the CSE and the apparent formation of polar outflows as the result of collimation produced by the interaction between the circumstellar disc and a standard stellar wind.

In all cases, the radial extension of the outflows and the distance between separated patches are at the scale of some 100 au, a distance covered in 50 years at a velocity of 10 km·s^{-1}. Such a time scale is more than two orders of magnitude larger than the typical variability observed on the stellar disc. Whatever is causing these outflows to blow in a same direction over several years must have a lifetime at the same scale.

4.2. *Farther away*

A similar comment applies to the CSE's at larger distances, where the history of the mass-loss mechanism is explored at century scale. They are mostly studied using ALMA observations of the emission of CO lines, most SiO molecules having either been dissociated by UV radiation or adsorbed on dust grains. While covering the whole 4π solid angle, they display strong inhomogeneity and deviate significantly from spherical envelopes, taking rather the form of radially expanding oblate volumes more or less inclined with respect to the plane of the sky and hosting significant localised emission enhancements. Such are the cases of R Dor [52, 57, 59, 63], L$_2$ Pup [49] and possibly o Cet [54, 55]. The oblate CSE of R Dor (Figure 7) displays enhanced emissions in two back-to-back directions, each dominated by a pair of cores. The CSE of L$_2$ Pup probes the mass-loss history preceding the 1994 dimming event and hosts three directions of enhanced emission. The CSE of EP Aqr [30, 62, 64] is characterised by broad bipolar outflows along the disc axis, the two-component morpho-kinematics being clearly revealed by the Doppler velocity spectrum (Figure 8); a recently proposed interpretation assumes that it is the interaction of a standard wind with the circumstellar disc that causes the wind expansion velocity
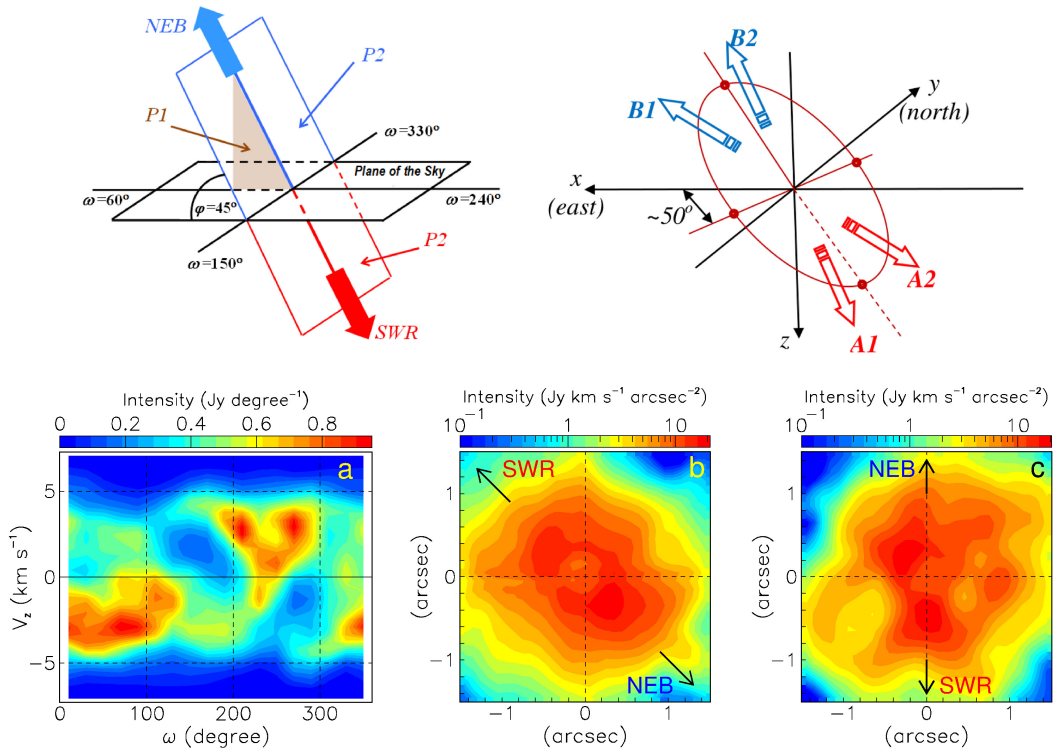
Figure 7. R Dor CSE. Upper panels: schematic of the morpho-kinematics [57]. Lower panels, SO(6_5–5_4) line emission [52]: (a) intensity in the Doppler velocity V_z vs position angle ω plane integrated over 12 au $< R <$ 60 au; (b) intensity projected on P1; (c) intensity projected on P2; planes P1 and P2 are defined in the upper-left panel. In both panels (b) and (c) NEB stands for north-east-blue-shifted and SWR for south-west-red-shifted and a cut $R >$ 0.3 arcsec (18 au) has been applied.

to decrease from ~10 km·s^{-1} on the disc axis down to ~2 km·s^{-1} in the disc plane, producing the appearance of two polar outflows [53]. Very patchy emission is observed in the CSEs of R Leo and *o* Cet (Figure 9). In the cases of R Leo [51] and R Dor [57], episodes of enhanced mass loss are revealed by elliptical depressions of the observed emission in the V_z vs R plane. The observed terminal velocities (Table A1) never exceed ~12 km·s^{-1}, reaching such a value in the only case of the bipolar outflows of EP Aqr, for which the terminal expansion velocity of the circumstellar disc is only ~2 km·s^{-1}; the mean terminal velocity of the five other stars is 5.4 km·s^{-1} with a rms deviation of only 0.8 km·s^{-1} with respect to the mean.

It is tempting to infer from these observations that whatever is causing ejection of gas from the extended atmosphere of the star, as do probably shocks induced by pulsations and convective cells, while displaying rapid variations at the scale of months, retain a same broad deviation from sphericity at century scale. However, such a conclusion is weakened by the remark that other mechanisms contribute to shaping the CSE away from the star. Such is particularly the case of the presence of stellar or planetary companions. In the present sample, the case of EP Aqr is the most compelling [53], the presence of polar outflows being understood as resulting from effective collimation by the continuous formation of a slowly expanding circumstellar disc.
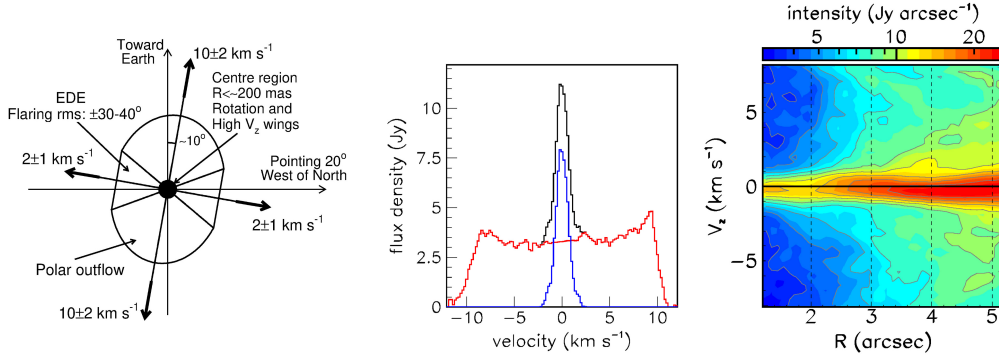
Figure 8. EP Aqr. Left: schematics of the morpho-kinematics of the CSE. Middle [64]: two-component structure of the Doppler velocity spectra of ^{13}CO(3–2) emission. The narrow component (equatorial density enhancement) is shown in blue and the broad component (bipolar outflow) in red. Right: PV map in the V_z vs R plane of the projection of the data cube defined as $1.2 < R < 5.2$ arcsec (140 to 620 au) and $|V_z| < 8$ km·s^{-1}.
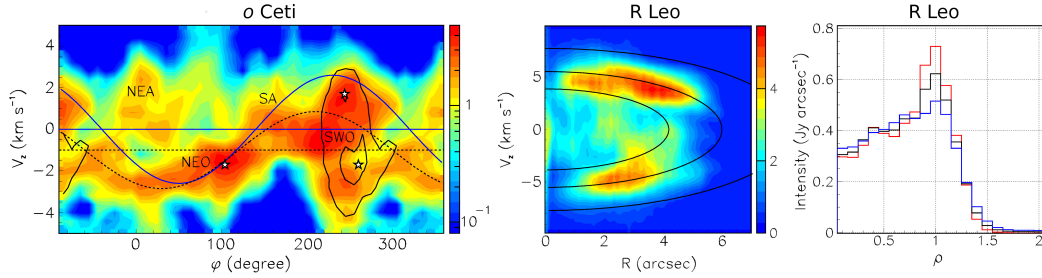

Figure 9. Left: the *o* Cet emissions of the CO(3–2) (colour) and SiO(5–4) (contours) lines integrated over $1.0 < R < 3.7$ arcsec (100 to 370 au) are shown in the Doppler velocity V_z vs position angle φ plane [55]. The colour scale is in Jy. NEA, SWO, SA and NEO stand for outflows identified in other projections of the data cube. The full (dashed) sinusoidal lines are the traces of an isotropic radial wind of 2.8 (2.0) km·s^{-1} velocity blowing in the plane of Mira B orbit using systemic velocities of 47.7 (46.7) km·s^{-1}. Middle: the R Leo emission of the CO(2–1) line [51] integrated over the position angle and displayed in the Doppler velocity vs R plane gives evidence for enhanced emission in a shell emitted 5 to 6 centuries ago. The lines show ellipses $\rho = 1/\sqrt{2}$, 1 and $\sqrt{2}$ with $\rho = ([V_z/5.5 \text{ km/s}]^2 + [R/6''])^2)^{1/2}$. The right panel displays the dependence on ρ of the intensity integrated over each of the blue- and red-shifted hemispheres separately as well as over the whole range of Doppler velocities (blue, red and black respectively).

5. High Doppler velocity wings and possible rotation in the inner CSE layer

5.1. *General comments*

All six stars give evidence for significant effective line broadening, in particular of SiO lines, at distances from the star below ~15 au, the less convincing case being of W Hya, for which clear line broadening is only seen over the stellar disc. It is observed in the form of high Doppler velocity wings above continuum level and confined to the vicinity of the line of sight crossing the star at its centre; they extend to some ±10–20 km·s^{-1} in velocity and to some 15 au in radius.

They receive negligible contributions from thermal broadening and are understood as being in fact the result of the simultaneous observation of high-velocity blue-shifted and red-shifted gas flows on an angular scale smaller than the beam size. We recall that the maximal distance reached by a volume of gas launched with velocity V_0 at distance r_0 is $r_{\max} = r_0 V_{\mathrm{esc}}^2 / (V_{\mathrm{esc}}^2 - V_0^2)$ where the escape velocity $V_{\mathrm{esc}} = (2GM/r_0)^{1/2}$, G being Newton's gravity constant and M the mass of the star. Namely for a radial boost of velocity at the star photosphere equal to a fraction f of the escape velocity, it will reach $1/(1-f^2)$ stellar radii: it remains below ~5 stellar radii for $f < 0.9$ and then blows up rapidly when f approaches unity. For a solar mass star of radius 1 au, the escape velocity is 42 km·s^{-1} and a 20 km·s^{-1} boost will therefore produce a maximal distance of ~1.3 stellar radii.

The presence of high velocity wings had been noticed early in single dish observations [65], suggesting that the emission occurs close to the star, where SiO grains have not yet fully formed, and is somehow related to star pulsations. Their ALMA observation was first mentioned by Decin *et al.* [6] and early attempts at interpreting them as bipolar gas streams flowing along the line of sight in the case of EP Aqr [66] or as the effect of rotation in the case of L$_2$ Pup [20, 61] have been published. However, it has been later understood, following the study of other stars, that they are in fact confined to the close neighbourhood of the star and are essentially radial, although occasionally combining with rotation [53, 67]. As first remarked by Decin *et al.* [6], it is the high sensitivity of ALMA observations, rather than their high angular resolution, which made it possible to reveal their presence. Indeed, to the extent that their source is confined to the close neighbourhood of the star and that no other source of such high Doppler velocities exists, low angular resolution observations are able to detect them as long as their sensitivity is sufficient: their emission is a minor fraction of the total emission detected within the broad beam, but they have no competition in the extreme Doppler velocity region that they populate. That does not mean that high angular resolution observations are unnecessary. They are indeed essential to measure the radial extension of the source and to explore the details of its morphology projected on the plane of the sky.

Even with an excellent angular resolution, the observed line profile receives contributions from all sources located on the line of sight; the opacity of the layers crossed at the line frequency suppresses part of their emission but, at extreme Doppler velocities, the density can be expected to be low enough for absorption to be small. Several effects contribute to the dependence of the line emission on radial distance: depletion of the gas phase by adsorption on dust grains, as is the case for SiO and AlO; mode of excitation, by collision with other molecules, mostly hydrogen, or absorption of stellar UV radiation; photodissociation by interstellar radiation or by radiation emitted by the star itself or by a nearby white dwarf companion; dissociation produced by possible shocks; dependence on temperature, the relevant parameters being the emission parameter ε, which measures the emissivity in the absence of absorption, and the optical depth τ.

Absorption, particularly strong over the stellar disc but also extending well beyond it in some cases (see Section 3), complicates the study of line broadening, the line profile being interrupted over a significant interval of Doppler velocity. Its contribution needs to be taken in a proper account. The complexity of the physics mechanisms at stake is particularly well illustrated by the analyses of Wong *et al.* [25] for o Cet and Vlemmings *et al.* [29] for W Hya.

Evidence for rotation in the inner region of the CSE, at distances from the star comparable with those covered by significant effective line broadening, has been found in four stars of the present sample, particularly strong in L$_2$ Pup and R Dor, but absent in W Hya and R Leo.

The presence of rotation in the same radial range as line broadening requires disentangling the two effects, which can be done by considering separately four quadrants of position
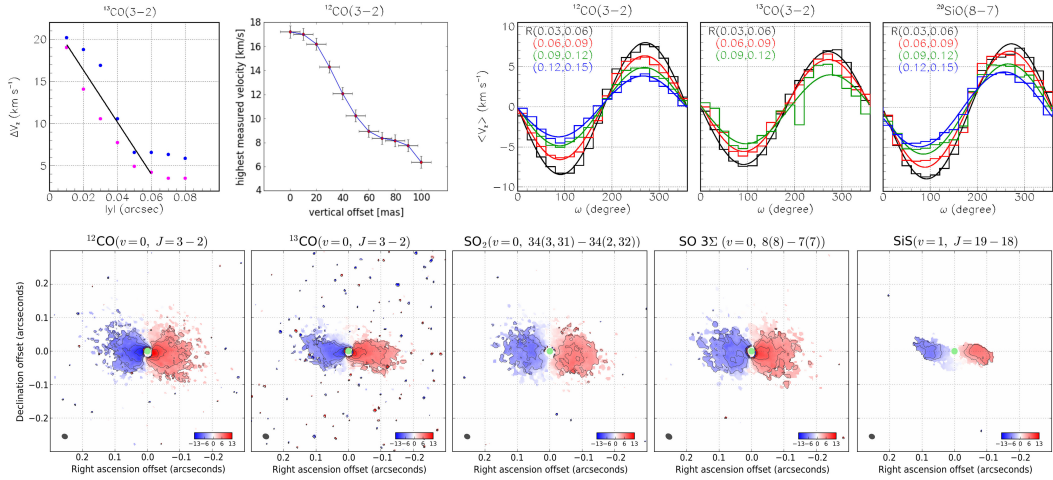
Figure 10. Upper row, left pair of panels: line broadening in L_2 Pup measured on the *y* axis where contribution from rotation cancels as seen from ^{13}CO(3–2) line emission (left, [49]) and ^{12}CO(3–2) line emission (right, [61]); the left panel shows the evolution of the FWHM line width (blue and red correspond to south and north, respectively) and the right panel the maximal velocity. Upper row, right triplet of panels: L_2 Pup [49], dependence on position angle of the Doppler velocity averaged over $|V_z| < 20$ km·s^{-1} in successive rings as indicated in the inserts (in arcsec); the lines show sine wave fits. Lower row: maps of the mean Doppler velocity measured for several L_2 Pup lines observed with high angular resolution by Kervella *et al.* [20].

angle: near the projection of the rotation axis on the plane of the sky, the effect of rotation cancels, while it is maximal in the perpendicular direction. Similarly, the possible presence of expansion in this radial range complicates the analysis of the line broadening and needs to be properly taken into account. A detailed discussion of disentangling the effects of line broadening, rotation and expansion has been given by Nhung *et al.* [67] using the case of R Hya as an illustration.

5.2. *Selected sample*

5.2.1. *L_2 Pup*

Hoai *et al.* [49] and Homan *et al.* [61] have given evidence for high $|V_z|$ wings in the ^{29}SiO(8–7) and ^{12,13}CO(3–2) emissions of the inner CSE of L_2Pup: over ~60 mas (3.8 au) from the centre of the star, the effective line width increases (FWHM) from ~5 km·s^{-1} to ~20 km·s^{-1} (Figure 10, upper row). The rotation of the gas and dust disc is seen on all observed lines (Figure 10, lower row) with a projected rotation velocity increasing from ~4 km·s^{-1} to ~8 km·s^{-1} (Figure 10, upper row) when *R* decreases from 120–150 mas to 30–60 mas [49]. However, ignoring line broadening, Kervella *et al.* [20] claim instead a projected rotation velocity of ~15 km·s^{-1} in the 30–60 mas interval.

5.2.2. *o Cet*

Hoai *et al.* [55] and Nhung *et al.* [54] give strong evidence for the line width of the SiO emission to increase from $|V_z| \sim 5$ km·s^{-1} to ~20 km·s^{-1} when *R* decreases from ~0.17 to ~0.05 arcsec (17 to 5 au) and for rotation about an axis projecting 40°±15° east of north with a projected velocity of
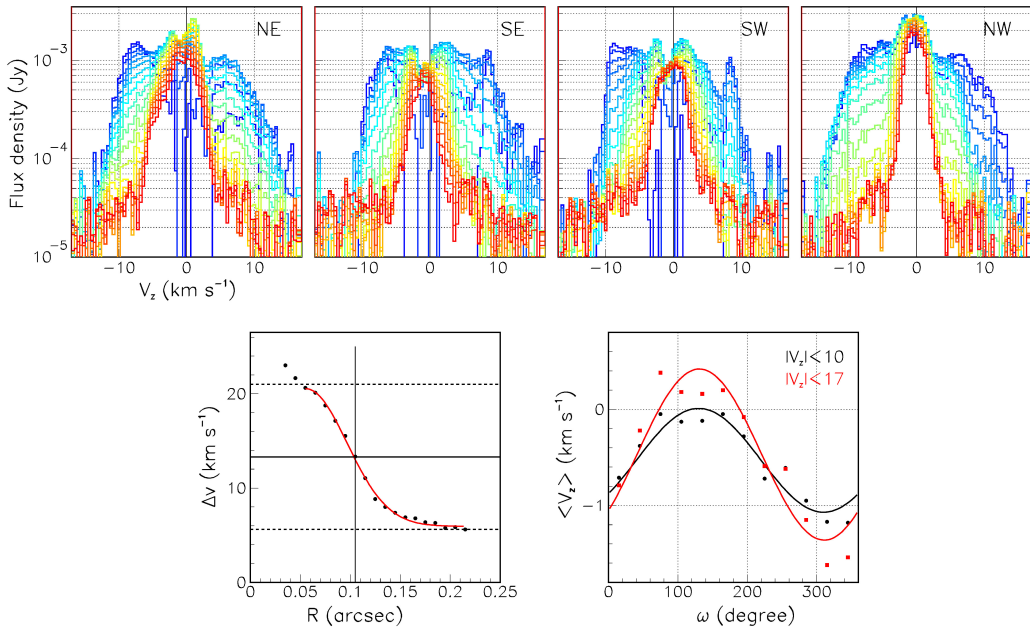
Figure 11. Line broadening and rotation in the SiO(5–4) line emission of *o* Cet [54, 55]. Upper row: Doppler velocity spectra averaged in quadrants of 3 au broad annular rings centred on Mira A with mean radii increasing from 2.5 au (blue) to 21.5 au (red) in steps of 1 au. The dependence on *R* of the full-width at 1/5 maximum of the spectra is shown in the lower-left panel. Lower right: dependence of the mean Doppler velocity on position angle ω in the ring 3 au < *R* < 10 au. The lines are sine wave best fits.

0.7 ± 0.2 km·s^{-1}, in agreement with results obtained from the observation of SiO masers [68, 69]. The low rotation velocity and the absence of absorption outside the stellar disc make this case relatively easy to analyse (Figure 11).

5.2.3. *W Hya*

The study of line broadening in W Hya [29, 50] is made difficult by the presence of a recent mass ejection in the blue-shifted northern octant; outside the region of the sky plane covered by this mass ejection, observations of the ^{29}SiO(8–7) line emission using a 45 mas (4.7 au) FWHM beam show that the largest Doppler velocities are observed within ~75 mas (7.8 au) projected distance from the centre of the star and reach only ~10 km·s^{-1}, less than twice the terminal velocity. The clearer evidence for larger Doppler velocities is from the absorption spectra measured over the stellar disc, reaching ~ ±20 km·s^{-1} and showing evidence for in-falling gas reaching high Doppler velocity. Vlemmings *et al.* [29], using a beam of only ~16 mas FWHM, have observed the CO(ν = 1,3–2) line emission of W Hya, which, with an upper level at 3120 K, probes efficiently the warm extended atmosphere. Their analysis reveals the presence of a warm molecular layer close to the stellar surface, with temperatures nearing 3000 K, surrounded by a cooler layer at ~900 K, extending to radial distances of ~50 mas and hosting both infall and outflow components (Figure 12). These reach larger velocities in the eastern hemisphere than in the western hemisphere where a hot spot of continuum emission is observed. No evidence for rotation has been reported.
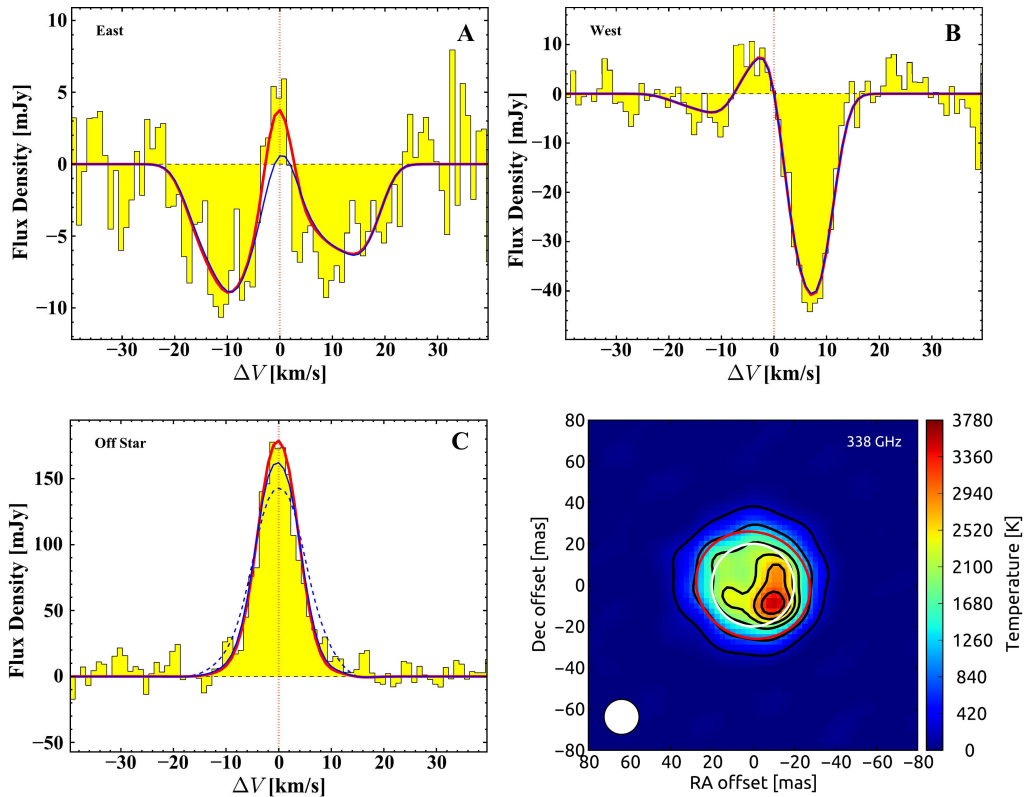
Figure 12. Doppler velocity spectra of the CO($v = 1,3–2$) line emission of W Hya [29] extracted towards the eastern (A) and western (B) stellar hemisphere as well as in an annulus between 2.9 and 5 au off the star (C). The beam size is ~16 mas FWHM and the spectral resolution ~1 km·s^{-1}. The red lines show model results. The lower-right panel maps the brightness temperature of the stellar surface as observed with ALMA continuum emission at 338 GHz. The rms noise in the image is 18 K and the peak is 3560 K. The red ellipse indicates the size of the fitted, uniform, stellar disc with a brightness temperature of 2495 ± 125 K. The effective temperature of the photosphere is ~2500 K.

5.2.4. *R Leo*

In the case of R Leo, Hoai *et al.* [51] observe Doppler velocities reaching beyond 10 km·s^{-1} over the stellar disc for the ^{29}SiO(5–4), CO(2–1) and SO(5_5–4_4) lines. They decrease to ~10 km·s^{-1} for R between 30 and 50 mas (3.4 and 5.7 au) and reach terminal values of ~5 km·s^{-1} for R beyond ~100 mas (11.4 au). They show significant anisotropy, with stronger emission in the southern than the northern hemisphere. Fonfría *et al.* [70] have observed the emission of the CO(2–1) and ^{29}SiO(5–4) lines over the stellar disc (Figure 13) giving evidence for in-falling gas in front of the star and for most of the emission coming from directions that do not enclose the star; they comment on the possibility for the ^{29}SiO($v = 1,6$–5) line to show maser emission. They argue that the red-shifted absorption may be produced by radial movements of photospheric layers (or convective cells) due to the stellar pulsation and that the spectra suggest the presence of random gas movements in the stellar photosphere and/or of periodic shocks. They also suggest the possible presence of rotation, which, however, cannot be confirmed when the outflows described
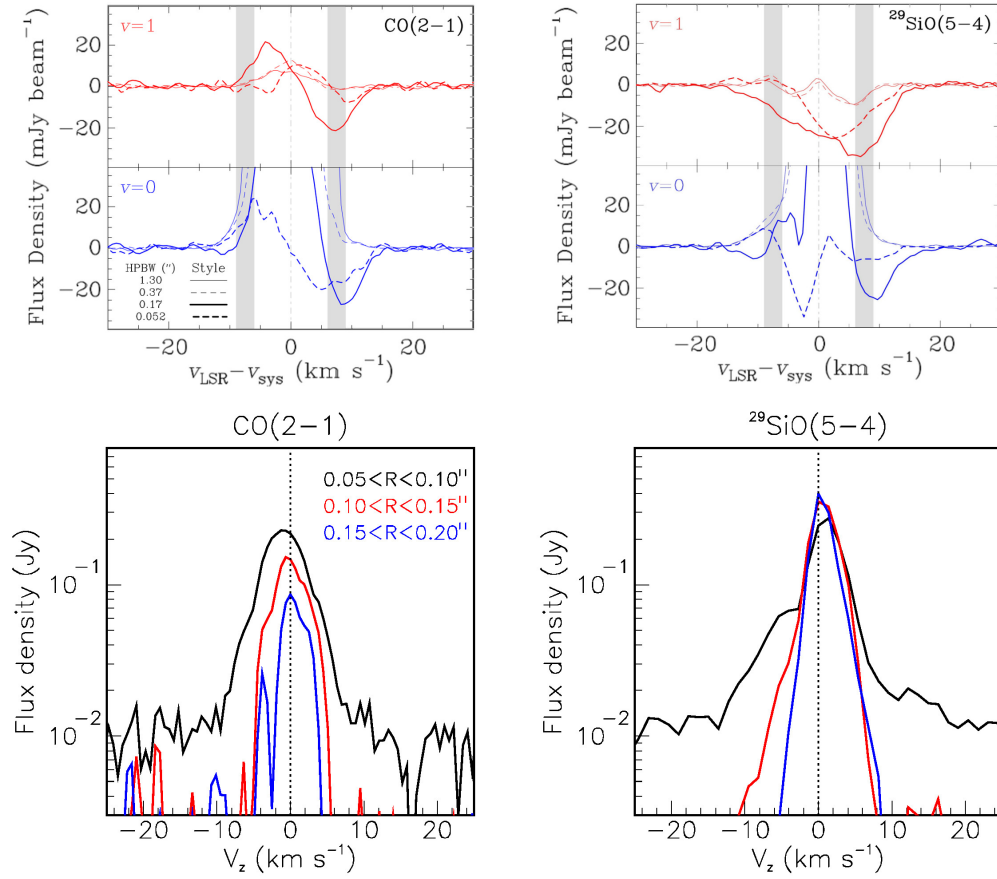
Figure 13. High velocity wings in R Leo. Upper pair of panels: Doppler velocity spectra [70] in the central pixel of the ^{12}CO(2–1) and ^{29}SiO(5–4) lines ($v = 0$ in blue and $v = 1$ in red). The different line styles correspond to different beam sizes as indicated in the insert. The grey vertical bands indicate the gas expansion velocity derived from single-dish observations. Lower pair of panels: Doppler velocity spectra [51] of the CO(2–1) and ^{29}SiO(5–4) line emissions in 50 mas (5.7 au) wide rings as indicated in the insert.

by Hoai *et al.* [51] are taken in due account. Higher angular resolution observations would be necessary to better explore the close environment of R Leo.

5.2.5. *R Dor*

In the case of R Dor, near the centre of the star, the presence of high Doppler velocity wings reaching 15–20 km·s^{-1} had been noted early by Decin *et al.* [6] and Hoai *et al.* [63] (Figure 14); Nhung *et al.* [52], using observations of the line emissions of ^{29}SiO(8–7) and SO$_2$(34$_{3,31}$–34$_{2,32}$) and accounting for the contribution of rotation, have shown that such a significant line broadening occurs within ∼12 au from the centre of the star. In this region evidence for rotation was first obtained by Vlemmings *et al.* [60] using high angular resolution observations of SiO($v = 3,5$–4), SO$_2$(16$_{3,13}$–16$_{2,14}$) and ^{29}SiO($v = 1,5$–4) emissions and, farther away from the star, by Homan *et al.* [59] using observations of the SiO($v = 1,8$–7) emission. The former authors gave evidence for solid-body rotation with velocity increasing from ∼1 km·s^{-1} near the stellar surface and the

Figure 14. R Dor inner CSE layer [52]. Left pair of panels: Doppler velocity distributions of the ^{29}SiO(8–7) emission observed for $|V_z| > 8$ km·s^{-1} using different datasets. Right pair of panels: dependence on positi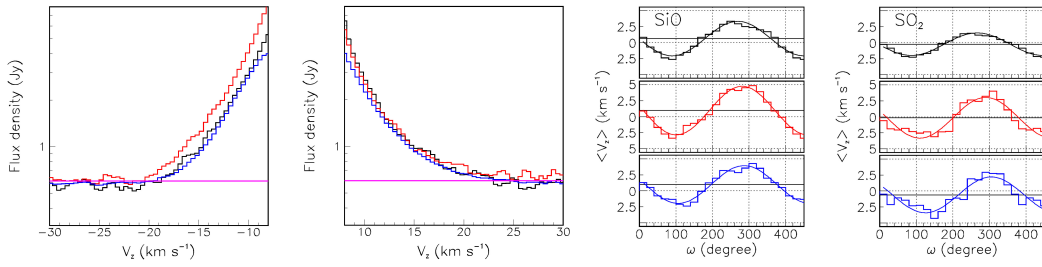on angle ω of the mean Doppler velocity averaged over $50 < R < 100$ mas (3 to 6 au, black), $100 < R < 150$ mas (6 to 9 au, red) and $150 < R < 200$ mas (9 to 12 au, blue) for ^{29}SiO(8–7) and SO$_2$($34_{3,31}$–$34_{2,32}$) line emissions.
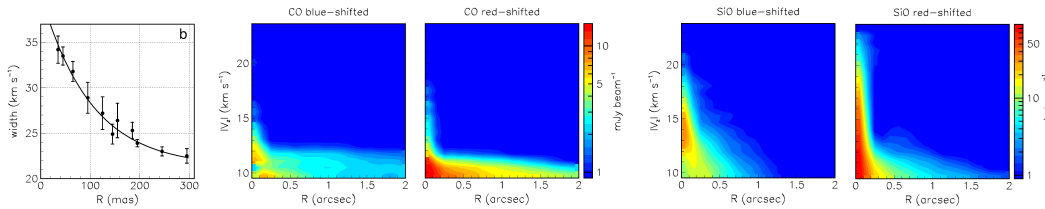
Figure 15. EP Aqr [53]. Left: radial dependence of the full width at 10% of the maximum of the Doppler velocity spectrum measured in a ring of radius R centred on the star. Four rightmost panels: PV maps of $|V_z|$ vs R for both hemispheres and both CO(2–1) and SiO(5–4) lines separately as indicated on top of each panel.

latter authors for sub-Keplerian rotation with velocity cancelling beyond 15 au from the centre of the star. Nhung *et al.* [52, 57] have later shown that rotation reaches a maximal velocity of ~5 to 7 km·s^{-1} at some 8 ± 2 au from the centre of the star, where the Keplerian orbital velocity around a solar mass star is ~11 km·s^{-1}. Its axis projects on the plane of the sky at a position angle of $10 \pm 5°$ and makes an unknown angle with the plane of the sky; yet, qualitative considerations favour a low value, typically $20° \pm 20°$ as suggested by the analysis of Homan *et al.* [59]. The morphology of the rotating volume does not show strong anisotropy and, in particular, fails to provide evidence for a disc-like flattening about the equator as observed in the case of L$_2$ Pup.

5.2.6. *EP Aqr*

High Doppler velocity wings, reaching ~$\pm$ 20 km·s^{-1}, have been observed [53] on both SiO(5–4) and CO(2–1) line emissions and shown to be confined within ~150 mas (18 au) from the centre of the star (Figure 15). The simultaneous presence of large radial wind velocities, reaching above 12 km·s^{-1} complicates their study. Evidence for rotation within some 100–200 mas (12 to 24 au) from the centre of the star, with a rotation velocity at km·s^{-1} scale, has been obtained from the observation of the emissions of the CO(2–1) and SO$_2$($16_{6,10}$–$17_{5,13}$) lines, consistent with observations of the dust induced polarisation of the 550–750 nm emission observed at the VLT using SPHERE-ZIMPOL [30]. This suggests that such rotation may be related to the precocious formation of the equatorial disc. Unfortunately, the orientation of the disc, inclined by only ~10° with respect to the plane of the sky, makes its study particularly difficult

and additional high sensitivity and angular resolution observations are necessary to clarify this point.

6. Discussion and conclusion

6.1. *Rotation and the role of planetary or stellar companions*

Evidence for rotation in the close neighbourhood of the star is generally ascribed to the presence of planetary or stellar companions. Indeed, while it is recognised that the initial angular momentum of the star must produce negligible velocities on the surface of the AGB star, which has expanded by over two orders of magnitude, planetary companions, whether orbiting the star above the photosphere or having been recently engulfed [71], can be expected to transfer a significant part of their angular momentum to the inner CSE. In contrast to protostars, the complex shock dynamics at stake near the photosphere is likely to prevent the radial distribution of the velocity of such rotating gas from being Keplerian. While some carbon-rich evolved stars, such as LL Pegasi [72], display very clear spiral features revealing the presence of a companion, oxygen-rich stars do not. Attempts at identifying such structures have always proven difficult. A well-documented recent example was given by Randall *et al.* [73] in the case of GX Monocerotis. In the particular sample of nearby stars considered in the present article, claims for the presence of spiral structures have been made by Ramstedt *et al.* [74] in the case of *o* Cet and by Homan *et al.* [30, 62] in the case of EP Aqr. However, the former has been shown by Hoai *et al.* [55] to wind in the wrong direction and serious doubts have been shed by Nhung *et al.* [53] on the reality of the latter. While the validity of the observation of possible spiral structures must be critically assessed, the failure to obtain reliable evidence should not be understood as a denial of the presence of planetary companions, which are obviously expected to be there. The question, which has currently received no satisfactory answer, is of their precise role in the generation of the wind. In the present sample, the only star, which has a well-established companion, in this case probably a white dwarf (Mira B), is *o* Cet. It plays a clear, but modest, role in focusing the wind of the main star [54, 55].

The case of EP Aqr is outstanding. The evidence for the precocious formation of a nearly face-on circumstellar disc is strong, the disc interacting with the nascent wind, giving the CSE its two-component appearance, with a pair of polar outflows. In such a case, the question to be answered is not the nature of the generation of the wind, assumed to obey the current state-of-the-art ideas developed in the current model, but the mechanism that governs the formation of the disc, which is unknown but might very well imply the presence of a planetary companion near the photosphere.

In the present sample, the two stars, which display clearer evidence for significant rotation, are R Dor and L_2 Pup. In the former case [52, 60, 62], rotation reaches a maximal velocity of ~6 km·s^{-1} at some 4 stellar radii from the centre of the star, and cancels beyond ~8 stellar radii, suggesting the presence of a planetary companion close to the photosphere or having been recently engulfed. The lack of significant oblateness disproves the presence of a thin circumstellar disc. There is no apparent relation between the geometry of the rotation (an axis projecting ~10° east of north on the plane of the sky) and that of the median plane of the global CSE (with a normal projecting ~120° east of north), probably implying that the observed rotation does not play an important role in the formation of the nascent wind.

The case of L_2 Pup [20, 49, 61] is different: the rotating volume is a nearly edge-on disc of gas and dust covering radial distances between 30 and 400 mas (2 to 26 au) from the centre of the star and rotation velocities reaching ~8 km·s^{-1} near the inner rim (the latter evaluation taking proper account of the effective line broadening in the vicinity of the star). As a result, at strong

variance with the disc of EP Aqr, the velocities are accurately measured but the radial distribution is not. This makes it difficult to compare the two circumstellar discs. The L_2 Pup disc seems, however, to be of a different nature: its outer diameter is much smaller, it hosts line emissions from both CO and SiO molecules while the EP Aqr disc is formed near the photosphere, where it is revealed exclusively by the emission of CO molecules and extends to large distances; in contrast with the EP Aqr disc, the L_2 Pup disc does not seem to play a role in shaping the CSE: farther away from the star, the wind oblateness is unrelated to the orientation of the disc and no evidence has been found for outflows collimated by the disc. This implies that for L_2 Pup, as for R Dor, the observed rotation does not play an important role in the formation of the nascent wind. But understanding the mechanism that governed the formation of the rotating circumstellar disc is complicated by the presence of the strong dimming episode that the light curve underwent at the end of the past century, inviting different speculations. Yet, it is generally assumed that an orbiting planetary companion is responsible for the observed rotation and Kervella *et al.* [20] claim to have obtained evidence for it, although their analysis suffers from ignoring effective line broadening.

In summary, while rotation is present within a few stellar radii of the centre of several oxygen-rich AGB stars, there is no evidence for it to play an important role in the generation of the nascent wind. There is no reason to doubt the presence of planetary companions orbiting AGB stars at short distances from their centre or having been recently engulfed, but their role seems limited to their impact on shaping the gravity field and to the production of rotation by dragging gas, with no significant incidence on the generation proper of the nascent wind. When based on the observation of an apparent spiral wake, claiming evidence for the presence of a companion requires a critical analysis, sufficiently rigorous to be credible. Cases where the presence of a companion is well established, such as *o* Cet in the present sample or R Aqr [75–77] and π^1 Gru [78] may display spectacular symbiotic phenomena, but the role of the companion is limited to its impact on shaping a pre-existing wind, with no incidence on its preliminary formation. Yet, more detailed studies of the mechanism governing the formation of rotation in the inner layers of the CSE, complicated by the presence of effective line broadening, are required in order to better specify the role played by possible companions.

6.2. *Effective line broadening and the role played by stellar pulsations and convective cell partition*

The commonly accepted ideas of the current model about the mechanisms governing the formation of the nascent wind of oxygen-rich AGB stars, outlined in the Introduction, are proving very useful in guiding current research and helping with the interpretation of the results. They have not suffered any significant contradiction. Yet, their validity is far from being confirmed and their conformity with observations is mostly qualitative.

Indeed, the present ALMA observations may suggest identifying the region where the wind gets its initial boost within the radial range over which effective line broadening is observed. The complexity of the morpho-kinematics at stake in this region is described by essentially just two numbers: its mean radius, measured from the centre of the star, r_{boost}, and the extreme velocity reached by the high V_z wings, V_{boost}. Table 1 lists their values together with the terminal velocity V_{term}, the stellar radius r_{star} and the mass-loss rate, $\dot{M}$. The values and uncertainties retained for W Hya, $V_{boost} = 15 \pm 5$ km·s^{-1} and $r_{boost} = 40 \pm 30$ mas (4.2 ± 3.1 au) reflect the difficulty to summarise in only two numbers the complex morpho-kinematics revealed by Vlemmings *et al.* [29] and Hoai *et al.* [50]. As illustrated in Figure 16, the values of V_{boost} are similar, with a mean value of 15.3 km·s^{-1} and a rms deviation of 2.6 km·s^{-1} with respect to the mean. The case of EP Aqr is outstanding, with a value of V_{term} (12 ± 2 km·s^{-1}) more than twice that of the other
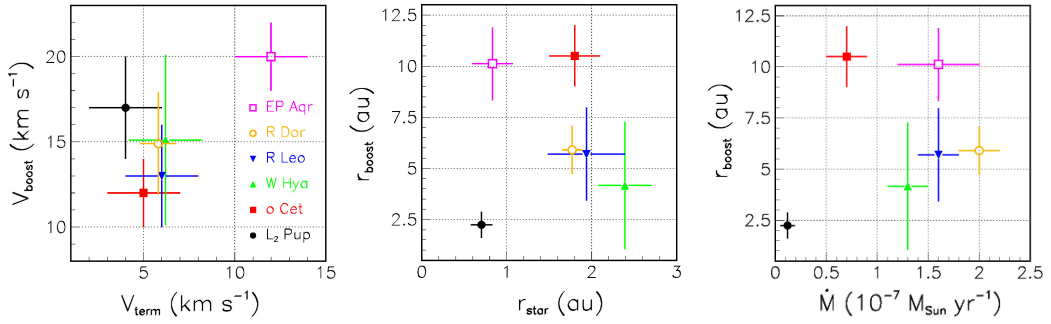
Figure 16. Location of the stars of the selected sample in the V_{boost} vs V_{term} (left), r_{boost} vs r_{star} (centre) and r_{boost} vs $\dot{M}$ (right) planes.

Table 1. Parameters of relevance to the region of effective line broadening

	L_2 Pup	o Cet	W Hya	R Leo	R Dor	EP Aqr
V_{boost} (km·s^1)	17 ± 3	12 ± 2	15 ± 5	13 ± 3	15 ± 3	20 ± 2
V_{term} (km·s^1)	4 ± 2	5 ± 2	6 ± 2	6 ± 2	6 ± 1	12 ± 2
r_{boost} (au)	2.2 ± 0.6	10.5 ± 1.5	4.2 ± 3.1	5.7 ± 2.3	5.9 ± 1.2	10.1 ± 1.8
r_{star} (au)	0.7 ± 0.1	1.8 ± 0.3	2.4 ± 0.3	1.9 ± 0.5	1.8 ± 0.1	0.8 ± 0.2
d (pc)	~64	~100	~104	~114	~59	~119
$\dot{M}$ (10^{-7} M$_{Sun}$/year)	0.12 ± 0.07	0.7 ± 0.2	1.3 ± 0.2	1.6 ± 0.2	2 ± 0.2	1.6 ± 0.4

stars of the sample (5.4 ± 0.8 km·s^{-1}) and a ratio $r_{boost}/r_{star} \sim 12$, four times as large, resulting from a very small stellar radius, ~7 mas (0.8 au), and a relatively broad line broadening region, reaching over 150 mas (18 au) from the centre of the star. For the other stars, r_{boost} increases in near proportion to r_{star}, with a ratio $r_{boost}/r_{star} \sim 3$; it is higher for o Cet, probably because of the larger mass of the star causing the mass-loss rate to be small in spite of the large value of r_{boost}. L_2 Pup, with the smallest values of both r_{boost} and $\dot{M}$, stands out as being particularly quiet. The crudeness of these considerations prevents us from making deeper comments and illustrates well the oversimplification implied by such description.

Ideally, one would like to tell apart, in correlation with the oscillations of the light curve, regions of the stellar disc over which gas is in-falling from regions where it is outflowing. Such detailed information is still lacking, with the exception of W Hya [29] where it is, however, only partial. Available Doppler velocity spectra measured over the stellar disc lack a systematic study of their dependence over the stellar phase and the ratio between the diameters of the beam and of the stellar disc are often too large.

Nearly fifty years have elapsed since Schwarzschild [79] estimated the size of convective cells in red giants and mentioned the possibility that they might play a role in generating mass loss. Later, Templeton and Karovska [80, 81] and Kiss, Szabó, and Bedding [82] presented indirect evidence for granulation of the photosphere from Fourier analyses of the light curves. But it was only five years ago that Paladini *et al.* [11], using PIONIER on the VLT, presented clear evidence for the presence of large granulation cells on the surface of π^1 Gruis. Such evidence has also been obtained, using PIONIER and NARVAL, for the red supergiant Betelgeuse [12, 13] and, using the latter instrument, for o Ceti and χ Cygni [11, 19]. While it is still lacking for the six stars of the present sample, ALMA observations of the continuum emission and VLT observations

of the stellar disc and of its close surroundings have produced images of very high angular resolution, which support the validity of the general picture outlined by the current model. Yet, clear evidence for strong inhomogeneity has been obtained for only three stars of the sample, W Hya, *o* Cet and R Dor, and its relation with possible convective cell partition is not clear.

The study by Vlemmings *et al.* [29] of the stellar disc of W Hya and its immediate neighbourhood offers a remarkable example of inhomogeneity. The observation of continuum emission gives evidence for a small ($\sim 2 \times 3$ mas^2) spot having a brightness temperature in excess of $\sim$53,000 K, consistent with the temperature expected in a strong shock, correlated with a significant excess of in-falling gas seen from its CO($\nu = 1,3$–2) emission. Two years later, observations [26] using a broader beam (48×40 mas^2), while still giving evidence for strong inhomogeneity, did not see any trace of the hot spot. Ohnaka *et al.* [9, 33] using SPHERE/ZIMPOL observations at two epochs, have resolved three clumpy dust clouds at a projected distance of $\sim$1.4–2 stellar radii, displaying clear time variations (in particular formation of a new dust cloud and disappearance of an earlier one) and correlated with the recent mass ejection described by Hoai *et al.* [50].

The case of *o* Cet is not particularly convincing when considering only VLTI/AMBER observations [83] and ALMA observations [26] of continuum emission using a beam of 33×23 mas^2. However, Kaminski *et al.* [27], using ALMA observations of the emission of the AlO(6–5) line with a similar beam (33×24 mas^2), have given evidence for the presence of two strong blobs of emission, at projected distances of 2.9 and 4.4 stellar radii in the NNW and E directions, respectively, revealing in-falling AlO gas having inward velocity of 4 to 7 km·s^{-1}. However, these blobs show no obvious correlation with the outflows displayed in Figure 2.

In the case of R Dor, there is evidence for clumpy emission, both from continuum with a beam of 25×18 mas^2 [26] and from dust [35]. The continuum emission of L$_2$ Pup, observed by Kervella *et al.* [20] with a beam of 18×15 mas^2, displays some elongation along the dust disc with a western excess that the authors interpret as evidence for a planetary companion at 2.0 ± 0.2 au; but it shows no feature that might suggest the presence of granulation. SPHERE/ZIMPOL $\sim$650 nm observations of the disc of EP Aqr [30] show evidence for light scattered by an inclined dust disc, but the observed intensity fluctuations are too small to claim the presence of granulation. The continuum emission of R Leo, observed by Vlemmings *et al.* [26] with a beam of 19×19 mas^2, reveals the outward motion of a shock wave, but no sign of hot spots; other observations (VLTI/AMBER [83]; VLTI/MIDI [41]; VLTI/VINCI [40]) suggest the presence of inhomogeneity and variability, but without firm evidence.

In summary, while the general features displayed by ALMA continuum and VLT optical/infrared observations unanimously support a model where the presence of large convection cells play an essential role in the generation of shocks responsible for the observed effective line broadening, direct evidence for the existence of such convective cells is scarce. When inhomogeneity is observed, usually with significant variability, in the form of hot spots of emission on the stellar disc or of clumpy dust emission, relating it to the presence of convective cells remains speculative and a detailed understanding of such a relation is still lacking. New VLT and ALMA observations of high sensitivity and angular resolution are still required, in particular in relation with the stellar phase, to progress towards a more quantitative description.

6.3. *On the nature of the gas outflows*

An observation that suffers no exception is of the presence of a reservoir of molecular gas gravitationally bound to the star within $\sim$2 stellar radii from its centre. As remarked by Vlemmings *et al.* [29] for W Hya, its total mass is over three orders of magnitude larger than the mass lost by the star in the course of one pulsation period. Thus, the gas spends at least 10^3 years in this region

or even closer to the photosphere, in a shock-heated environment that significantly affects the chemistry at stake. In no case does gas escape from this reservoir in a spherical flow; it does it instead in the form of outflows covering typical solid angles at steradian scale and displaying radial distributions showing that they last several decades. An interpretation in terms of the current model would suggest associating each such outflow with a giant convective cell having a lifetime of several decades, which contrasts with the millimetre continuum and VLT observations of variability on a much shorter time scale. A similar concurrence of two different time scales was observed on Betelgeuse using spectro-polarimeter observations [13]. In some cases, as for W Hya and R Leo, the global morphology of the CSE displays modest anisotropy, suggesting that on a time scale of centuries the outflows might be emitted over 4π steradians and anisotropy might somewhat average out. This may also be the case of EP Aqr, for which the interaction of the wind with the circumstellar disc dominates and prevents a reliable evaluation. In the cases of the higher mass-loss rate, R Dor, and of the lower mass-loss rates, o Cet and L_2 Pup, the global CSE seems to retain significant anisotropy, possibly related to the orbit of Mira B in the case of o Cet.

Smaller and more episodic outflows, as observed in o Cet, are more prone to dissociation by interstellar UV radiation, causing SiO abundance, in contrast to CO abundance, to be confined near the star. Nhung *et al.* [54] have discussed this issue in some detail but presently available observations do not allow for a reliable conclusion to be reached.

Other outflows seem to be of a different nature, looking more like mass ejections occurring over a short period of time. An extreme case is the mass ejection, which followed the magnetic flare that produced a soft X-ray burst in o Cet in 2003 [56]; this seems, however, to be rather the exception. It is not clear whether the mass ejections observed on W Hya (left panel of Figure 5) and on R Dor (right panel of Figure 4), which look like having occurred recently over a short period of time, are of a same or different nature as the former outflows; in particular, it is not clear whether they should be described in the framework of the same hydrodynamical models. More generally, these remarks raise the question of a possible continuity, as opposed to a completely different nature, between the mass ejection observed in o Cet in 2003 and the outflows observed in the other stars of the sample. Granulation, magnetic flares and coronal mass ejections are related phenomena and, in the case of the Sun, the details of these relations are still raising unanswered questions [84].

6.4. *Magnetic fields*

The generally accepted picture described by the current model offers a framework in which to study the role played by magnetic fields in generating the nascent wind and, later, shaping it towards the planetary nebula phase. While little is known about such a possible role [85], the presence of magnetic fields near the stellar surface has been suggested by events such as UV emission from a majority of AGB stars [86], the occurrence of a soft X-ray outburst on o Cet [56] or the ephemeral presence of a small and very hot spot on the surface of W Hya [29]. An abundant literature addresses topics of direct relevance to the role possibly played by magnetic fields in relation to convections, pulsations and shock waves [14, 28, 87–91], illustrating the importance of devoting to it increased observational attention.

Of direct relevance to the present sample of selected stars are measurements and observations made on o Cet, W Hya and R Leo. Significant polarisation of maser emission from vibrationally excited SiO lines [68, 69, 92, 93] has been measured using VLBA observations, complemented by VLTI/MIDI interferometry at 10 μm wavelength, and 30 m IRAM single dish observations. While giving clear evidence for the presence of magnetic fields of a few Gauss, they are difficult to interpret in terms of their structure, radial or toroidal. Recently, using CARMA observations, Huang *et al.* [94] have measured linear polarisations from the Goldreich–Kylafis effect on the

CO(2–1) emission of R Leo at the level of ~9.7%. The effect reveals unequal populations of the sublevels of the final state of the transition and gives reliable evidence for the presence of magnetic field. Finally, using NARVAL mounted on the 2 m telescope at Pic du Midi Observatory, Fabas *et al.* [28] have observed variability and structures on the polarised Balmer line emission of *o* Cet, which they interpret in terms of shock waves suggesting the presence of magnetic field. Also worth mentioning is a magneto-hydrodynamic model of *o* Cet proposed by Thirumalai and Heyl [89], which describes how an equatorial magnetic field could contribute to the production of a dust-driven wind.

6.5. *Conclusion*

We have presented a brief review of the current knowledge of the properties displayed by the CSEs of a sample of six well-studied nearby oxygen-rich AGB stars. The aim has been to illustrate difficulties experienced when comparing observations with current models and possibly identify ways to overcome them, or at least to progress in such a direction. The scope of the article is accordingly limited, and we list below a few points of relevance in this respect.

(i) We use as reference the simulations published by Freytag, Höfner and coworkers (references 1 to 4). These should not be understood as one model out of many possible, but as providing a useful and convenient summary of the current understanding of the mechanisms governing the genesis of the wind, including pulsations, convections, shocks, dust formation and radiation pressure. We take it as granted that there is no question that these are indeed the main contributions to the genesis of the nascent wind. There exist, of course, many other publications addressing the issue from a theoretical or phenomenological point of view, but reviewing, or even simply mentioning these would not alter the general picture and is outside the scope of the present article.

(ii) One may find frustrating, or at least disappointing, that the many observations reported in the article, making use of the outstanding performance of instruments such as VLT or ALMA, leave so many questions unanswered. Their diversity, each star appearing as a singular case, makes it difficult to identify common features with confidence. Moreover, the intrinsic limitations inherent to astronomical observations, with only two position coordinates and a single velocity component being accessible to measurement, must be kept in mind: experience shows that when more accurate measurements become available, some of our earlier preconceptions may need to be abandoned, or at least modified. In such a context, it is important to clarify which are the main open questions and, if possible, to seek ways to progress towards answering them.

(iii) We have limited our study to M-type stars, oxygen-rich, having a small mass-loss rate and displaying no clear technetium signal. The occurrence of third-dredge-up events is obviously a major step in the evolution of AGB stars. It adds a further complication to the mechanisms governing the genesis of the nascent wind and would deserve being scrutinised in a separate study including the evolution to S-type and carbon stars. It leaves many new questions unanswered, such as why Tc-rich and Tc-poor stars populate different regions of the period-luminosity diagram [95, 96] or of a possible relation between third-dredge-ups and specific features of the light curves [97].

(iv) We have deliberately excluded considerations on the fate of the wind following its genesis, such as the nature of the superwind that precedes the formation of planetary nebulae, or the possible presence of spiral structures revealing the shaping of the wind by distant companions. It was usual, in the early literature, to assume that the wind was isotropic in the early stage of the AGB, and it was therefore natural to see such phenomena as being the cause of the breaking of spherical symmetry observed in planetary nebulae. But the

high angular resolution observations that instruments such as ALMA and VLT have now made possible have shown that spherical symmetry is in fact already broken in the early stage of the AGB, making it advisable to understand the genesis of the nascent wind at this stage before addressing its subsequent evolution.

In summary, we have identified a few domains that deserve particular attention and a continued, or even increased effort on both observational and phenomenological fronts:

(i) The role played by shocks. Their impact is important and one tends to blame them whenever an unexpected feature is observed. Yet, few observations allow for a reliable identification of the exclusive effect of shocks and, in particular, for a quantitative evaluation of its importance. A characteristic property of shocks is to induce a specific chemistry, a result of the very high temperatures that they are hosting. Shock chemistry allows for the production of molecules such as OH or HCN at rates very different from those possible without shocks [98–100]. An abundant literature addresses this topic and we mentioned in the text the case of OH molecules detected in the neighbourhood of W Hya and R Dor [48]. Systematic measurements of abundance ratios such as HCN/SiO close to the star would therefore help with understanding why they seem to play a significantly more important role in some stars than in others. Similarly, emission ratios from a same line allow for a quantitative evaluation of the deviation from LTE predictions and of the role played by shocks. An example is the SiO(5–4)/SiO(6–5) emission ratio predicted to be ~0.5 and measured in R Dor to be 0.77 [58]. Systematic measurements of such abundance and emission ratios would make it possible to look for correlations with other parameters characteristic of the star and should be encouraged.

(ii) The role played by stellar pulsations. Over four decades ago, Hinkle and coworkers presented an analysis of infrared spectroscopic observations of χ Cygni covering more than three periods of the light curve [101] and gave evidence for the presence of a wave driven by the stellar pulsation and travelling outward in the stellar atmosphere. Since that time, much progress has been achieved in understanding the role played by stellar pulsations in the generation of the nascent wind and in the study of the light curves of Mira's and Long Period Variables. Yet, correlated observations of the light curve and of either optical/infrared or millimetre emissions are scarce. This is very much lacking and should be given much more attention than it currently is. Moreover, a quantitative understanding of the ballistic up-down excursions experienced by the gas above the photosphere is also badly needed. As was illustrated in Section 6.2 and Figure 16, we are still a long way from it. Systematic very high-resolution measurements of the line broadening observed in the close neighbourhood of the star, together with careful analyses of Doppler velocity spectra above the stellar disc should be encouraged with the aim to reveal correlations with properties characteristic of the star.

(iii) The role played by convection cells. The evidence for convection cells to play an important role is strong and we had many opportunities to illustrate it. Yet, we fail to quantify critically the degree of agreement between observations and model simulations. Images of the star surface of the same quality as obtained on π^1 Gru [11] using PIONIER should be sought for other stars and a similar comment can be made concerning continuum maps of the same quality as obtained on W Hya using ALMA [29]. One tends to blame convection cells for any deviation from spherical symmetry at steradian scale: we need a more rigorous approach to the problem, in particular with understanding the diversity of time scales that seem to govern the variability of the observed properties. We fail to understand clearly what is causing the modulation of the gas outflow, both in time, with episodes of enhanced mass loss, and in space, with steradian like enhancements that we

tend to blame on convection cells. A considerable effort in obtaining many more high-resolution observations of the emission of several molecular lines is needed on a large sample of nearby stars in order to progress. In particular, as mentioned in the text, the precise nature of blobs of gas emission as observed in R Dor and W Hya needs to be clarified.

(iv) Rotation and disc formation. As we mentioned in the text, the question of what is the cause of the slow rotations observed near the surface of some stars, star rotation or close-by planetary companion, remains open. Moreover, what is causing the formation of a circumstellar disc on stars such as L_2 Pup, EP Aqr or RS Cnc needs to be clarified. This calls for an increased effort in high angular resolution observations of the emission of several molecular lines.

(v) Magnetic fields. As discussed in Section 6.4, we know of the presence of magnetic fields near the surface of some stars, but it seems that they do not play a significant role in the genesis of the nascent wind, at least in the early AGB phase discussed in the article. Yet, we need to be much clearer on this point than we currently are, but how precisely one should proceed is not clear to us.

(vi) Finally, one must keep in mind that the primary cause of the nascent wind is located inside the star, where nuclear reactions occur. Ultimately, we shall need to understand it before being able to claim that we understand the genesis of the wind. In this context, understanding the evolution of the stars from M to S and C types, including the precise role played by third-dredge-up events and by mixing is obviously essential.

The contribution of the present article to the progress of the field is both modest and limited in scope. It does not do more than illustrating the complexity of the issues that need to be addressed and of the problems that need to be solved. Such complexity calls for a multidisciplinary effort requiring familiarity with nuclear, atomic, molecular, plasma and condensed matter physics as well as with chemistry. This is highly challenging and we hope that the article has at least shed light on questions that need to be answered in priority in order to progress. The outstanding performance of the VLT and of ALMA in terms of angular resolution and sensitivity will still allow for major progress over many years to come.

Declaration of interests

The authors do not work for, advise, own shares in, or receive funds from any organization that could benefit from this article, and have declared no affiliations other than their research organizations.

Funding

Acknowledgements

MOST and ASIAA (Taiwan), and KASI (Republic of Korea), in cooperation with the Republic of Chile. The Joint ALMA Observatory is operated by ESO, AUI/NRAO and NAOJ. We are deeply indebted to the ALMA partnership, whose open access policy means invaluable support and encouragement for Vietnamese astrophysics.

Appendix A.

See Tables A1 and A2.

Table A1. Parameters and references of relevance to the six selected stars

	L_2 Pup HD56096	*o* Cet HD14386	W Hya HD120285	R Leo HD84748	R Dor HD29712	EP Aqr HD207076
Type (spectral /variable)	M5IIIe/SRb	M7-IIIe /Mira	M7.5-9/SRa	M7-9/Mira	M8/SRb	M7-8/SRb
d (pc)	64 ± 4 [102]	~100 [102]	104 [102]	114 [102]	59 [103]	119 [102, 104]
R_{star} (au) continuum/NIR	0.58/0.64 [45, 47]	2.1/1.5 [26]	2.7/2.1 [26]	2.4/1.6 [26]	1.9/1.7 [26]	1.0/0.7 [30, 105]
Period (d)	141 [42, 43]	333 [80, 81]	361 [106]	310 [107]	175/332 [108]	110 [109, 110]
Mass (M_{Sun})	~0.7 [20]	$A \sim 2.0$, $B \sim 0.7$ [111]	1.0–1.5 [112–114]	~0.7 [115]	0.7–1.0 [39]	~1.7 [30]
Mass-loss rate ($10^{-7} M_{Sun}$/yr)	0.12 ± 0.07 [49]	$0.7 \pm 0.2/2.5$ [54, 116]	1.3 [113, 114]	~1.6 [117]	~2 [58]	1.6 ± 0.4 [64]
Terminal velocity (km·s^{-1})	3.4 ± 1.7 [49]	2.5 [116]	5 [50]	5.5 [51]	6–9 [57]	2–11 [64]
VLT NACO VLTI VINCI	[45–47]		[36]	[36, 40]	[36]	
VLT SPHERE	[31]	[32]	[9, 33, 34]		[35]	[30]
VLTI AMBER	[47]	[83]	[9, 33, 37]	[83]	[39]	
VLTI MIDI	[45]		[38, 118]	[41]		
Others		[23, ISI], [24, IOTA] [119], [120, Keck] [121, ISI]	[119], [120, Keck] [122, ISO]	[123, IOTA] [119], [120, Keck] [124, SAO], [121, ISI]		
ALMA continuum	[20]	[21, 22, 25, 26] [27, 32, 111]	[26, 29]	[26]	[26]	[30]
ALMA and APEX Abundances		[27, 125]	[7, 48, 112, 126]		[5, 48, 127]	
ALMA molecular lines	[20, 49, 61]	[25, 32, 54] [55, 128, 129]	[7, 29, 50, 130]	[51, 70, 131]	[6, 52, 57, 59] [60, 63]	[30, 33, 62] [64, 66]
Others		[22, JVLA]		[132, VLA] [133, JVLA]	[58, APEX/SEPIA]	
Masers	[44]	[68, 69, 92, 134]	[92, 93, 122] [134, 135]	[68, 92, 93, 134] [136–138]		

Spectral and variability types are taken from standard catalogues [106, 139, 140]. Distance (d) measurements are typically reliable to within $\pm 10\%$, with the exception of R Leo for which we retain the Hipparcos value of 114 pc [102] rather than the Gaia value of 71 pc [141, 142]. Stellar radii (R_{star}) measurements span broad samples of values, depending on stellar phase and wavelength. We retain values [26] (continuum at millimetre wavelengths and near infrared) quoted in a reliable and critical review of four of the stars in our sample. For the other two stars (L_2 Pup and EP Aqr), the continuum values are poorly measured. The period of EP Aqr is poorly known and often quoted as 55 d while it is in fact more like 110 days. Masses are not precisely measured and are mostly crude estimates.

Table A2. Molecular lines observed and studied with high angular resolution (beam FWHM < ~200 mas) in the selected sample of six stars

Line	A [Hz]	E_{up} [K]	f [GHz]	L$_2$ Pup	o Cet	W Hya	R Leo	R Dor	EP Aqr
$^{12}C^{16}O(v=0,2\text{--}1)$	6.91×10^{-7}	16.6	230.5				40		25
$^{13}C^{16}O(v=0,2\text{--}1)$	6.04×10^{-7}	15.9	220.4						23
$^{12}C^{16}O(v=0,3\text{--}2)$	2.50×10^{-6}	33.2	345.8	21		46		160	
$^{12}C^{16}O(v=1,3\text{--}2)$	1.45×10^{-6}	3120	342.6			17			
$^{13}C^{16}O(v=0,3\text{--}2)$	2.18×10^{-6}	31.7	330.6	22					
$^{28}Si^{16}O(v=0,5\text{--}4)$	5.91×10^{-4}	31.3	217.1		32–45				24
$^{28}Si^{16}O(v=1,5\text{--}4)$	0.50×10^{-3}	1800	215.6		32		42		
$^{28}Si^{16}O(v=1,8\text{--}7)$	2.20×10^{-3}	1844	344.9				47	150	
$^{28}Si^{16}O(v=2,5\text{--}4)$	0.51×10^{-3}	3552	214.1		32		46		
$^{28}Si^{16}O(v=3,5\text{--}4)$	5.08×10^{-4}	5287	212.6					36	
$^{29}Si^{16}O(v=0,5\text{--}4)$	0.50×10^{-3}	30.9	214.4		32		46		
$^{28}Si^{16}O(v=0,8\text{--}7)$	2.20×10^{-3}	75.0	347.3					30	
$^{29}Si^{16}O(v=1,5\text{--}4)$	4.93×10^{-4}	1789	212.9					36	
$^{29}Si^{16}O(v=0,8\text{--}7)$	2.10×10^{-3}	74.1	343.0	20		35–45		30	
$^{30}SiO(v=0,8\text{--}7)$	2.05×10^{-3}	73.2	338.9					150	
$^{28}Si^{32}S(v=1,19\text{--}18)$	6.89×10^{-4}	1236	343.1	20					
$^{32}S^{16}O(5_5,4_4)$	0.12×10^{-3}	44.1	215.2				42		
$^{32}S^{16}O(6_5,5_4)$	1.96×10^{-4}	50.7	251.8					150	
$^{32}S^{16}O(v=0,8_8\text{--}7_7)$	5.19×10^{-4}	87.5	344.3	20					
$^{32}S^{16}O(v=0,8_9\text{--}7_8)$	5.38×10^{-4}	78.8	346.5					150	
$^{32}S^{16}O_2(34_{3,31},34_{2,32})$	3.45×10^{-4}	581.9	342.8					38	
$^{32}S^{16}O_2(16_{3,13},16_{2,14})$	9.90×10^{-5}	147.8	214.7					36	
$^{32}S^{16}O_2(16_{6,10},17_{5,13})$	2.35×10^{-5}	213.3	234.4						175
$^{32}S^{16}O_2(13_{2,12},12_{1,11})$	2.38×10^{-4}	92.8	345.3				47		
$^{32}S^{16}O_2(22_{2,20},22_{1,21})$	9.30×10^{-5}	248.4	216.6				42		
$^{32}S^{16}O_2(4_{2,2}\text{--}3_{1,3})$	7.69×10^{-5}	19.0	235.2						25
$H_2^{16}O(v_2=1,5_{5,0},6_{4,3})$	4.77×10^{-6}	3462	232.7		30				
$H^{12}C^{14}N(4\text{--}3)$	2.06×10^{-3}	42.5	354.5					151	
$H^{13}C^{14}N(4\text{--}3)$	1.90×10^{-3}	41.4	344.2				45		
$^{27}Al^{16}O(N=9,8)$	See [7]		344.4			34			
^{16}OH Many (see [48])						~30		~30	

Emission related parameters (Einstein coefficient A, energy of the upper level E_{up} and frequency f of the transition) are listed in the first columns. For each star the mean beam size (FWHM) associated with the highest angular resolution is listed in mas in the last columns. We recall that the emissivity ε and the optical depth τ are obtained from the relations $\varepsilon[\text{Jy}\times\text{arcsec}^{-2}]/N[\text{mol}\cdot\text{cm}^{-3}\cdot\text{arcsec}] = 5.5\times10^3 \times d[\text{pc}] \times A[\text{s}^{-1}]f_{pop}$ with $f_{pop} = k(2J+1)e^{-Eu/T}/T$ and $\varepsilon/\tau = 0.34\times10^{-7}f^3/(e^{\Delta E/T}-1)$ where N is the density, d the distance from Earth to the star and k is the product of the partition function by the temperature.

References

[1] B. Freytag, S. Liljegren, S. Höfner, "Global 3D radiation-hydrodynamics models of AGB stars; Effects of convection and radial pulsations on atmospheric structures", *Astron. Astrophys.* **600** (2017), article no. A137.

[2] S. Höfner, H. Olofsson, "Mass loss of stars on the asymptotic giant branch; Mechanisms, models and measurements", *Astron. Astrophys.* **26** (2018), article no. 1.

[3] S. Höfner, B. Freytag, "Exploring the origin of clumpy dust clouds around cool giants; A global 3D RHD model of a dust-forming M-type AGB star", *Astron. Astrophys.* **623** (2019), article no. A158.

[4] B. Freytag, S. Höfner, "Global 3D radiation-hydrodynamical models of AGB stars with dust-driven winds", *Astron. Astrophys.* **669** (2023), article no. A155.

[5] L. Decin, A. M. S. Richards, L. B. F. M. Waters *et al.*, "Study of the aluminium content in AGB winds using ALMA. Indications for the presence of gas-phase (Al$_2$O$_3$)$_n$ clusters", *Astron. Astrophys.* **608** (2017), article no. A55.

[6] L. Decin, A. M. S. Richards, T. Danilovich *et al.*, "ALMA spectral line and imaging survey of a low and a high mass-loss rate AGB star between 335 and 362 GHz", *Astron. Astrophys.* **615** (2018), article no. A28.

[7] A. Takigawa, T. Kamizuka, S. Tachibana *et al.*, "Dust formation and wind acceleration around the aluminum oxide-rich AGB star W Hydrae", *Sci. Adv.* **3** (2017), no. 11, article no. eaao2149.

[8] A. Takigawa, T.-H. Kim, Y. Igami *et al.*, "Formation of transition alumina dust around asymptotic giant branch stars: condensation experiments using induction thermal plasma systems", *Astrophys. J.* **878** (2019), article no. L7.

[9] K. Ohnaka, G. Weigelt, K.-H. Hofmann, "Clumpy dust clouds and extended atmosphere of the AGB star W Hydrae revealed with VLT/SPHERE-ZIMPOL and VLTI/AMBER", *Astron. Astrophys.* **589** (2016), article no. A91.

[10] S. Liljegren, S. Höfner, B. Freytag, S. Bradh, "Atmospheres and wind properties of non-spherical AGB stars", *Astron. Astrophys.* **619** (2018), article no. A47.

[11] C. Paladini, F. Baron, A. Jorissen *et al.*, "Large granulation cells on the surface of the giant star $\pi 1$ Gruis".

[12] M. Montargès, P. Kervella, G. Perrin *et al.*, "The close circumstellar environment of Betelgeuse. IV. VLTI/PIONIER interferometric monitoring of the photosphere", *Astron. Astrophys.* **588** (2016), article no. A130.

[13] A. López Ariste, P. Mathias, B. Tessore *et al.*, "Convective cells in Betelgeuse: imaging through spectropolarimetry", *Astron. Astrophys.* **620** (2018), article no. A199.

[14] A. López-Ariste, B. Tessore, E. S. Carlin *et al.*, "Asymmetric shocks in χ Cygni observed with linear spectropolarimetry", *Astron. Astrophys.* **632** (2019), article no. A30.

[15] G. Pojmanski, G. Maciejewski, B. Pilecki *et al.*, "Vizier online data catalog: asas variable stars in southern hemisphere", in *Vizier On-line Data Catalog: II/264*, 2005.

[16] S. J. Little, I. R. Little-Marenin, W. H. Bauer, "Additional late-type stars with technetium", *Astron. J.* **94** (1987), p. 981-995.

[17] A. D. Vanture, G. Wallerstein, J. A. Brown, G. Bazan, "Abundances of Tc and related elements in stars of type M, MS, and S", *Astrophys. J.* **381** (1991), p. 278-287.

[18] T. Kipper, "Technetium abundance in Omicron Ceti", *Baltic Astron.* **1** (1992), p. 190-193.

[19] T. Lebzelter, J. Hron, "A search for Technetium in semiregular variables", *Astron. Astrophys.* **351** (1999), p. 533-542.

[20] P. Kervella, W. Homan, A. M. S. Richards *et al.*, "ALMA observations of the nearby AGB star L_2 Puppis. I. Mass of the central star and detection of a candidate planet", *Astron. Astrophys.* **596** (2016), article no. A92.

[21] W. H. T. Vlemmings, S. Ramstedt, E. O'Gorman *et al.*, "Resolving the stellar activity of the Mira AB binary with ALMA", *Astron. Astrophys.* **577** (2015), article no. L4.

[22] L. D. Matthews, M. J. Reid, K. Menten, "New measurements of the radio photosphere of Mira based on data from the JVLA and ALMA", *Astrophys. J.* **808** (2015), article no. 36.

[23] A. A. Chandler, K. Tatebe, E. H. Wishnow *et al.*, "Asymmetries and outflows in the circumstellar dust of mira A", *Astrophys. J.* **670** (2007), p. 1347-1352.

[24] G. Perrin, S. T. Ridgway, S. Lacour *et al.*, "Evidence for localized onset of episodic mass loss in Mira", *Astron. Astrophys.* **642** (2020), article no. A82.

[25] K. T. Wong, T. Kamínski, K. M. Menten, F. Wyrowski, "Resolving the extended atmosphere and the inner wind of Mira (*o* Ceti) with long ALMA baselines", *Astron. Astrophys.* **590** (2016), article no. A127.

[26] W. H. T. Vlemmings, T. Khouri, H. Olofsson, "Resolving the extended stellar atmospheres of asymptotic giant branch stars at (sub)millimetre wavelengths", *Astron. Astrophys.* **626** (2019), article no. A81.

[27] T. Kamínski, K. T. Wong, M. R. Schmidt *et al.*, "An observational study of dust nucleation in Mira (o Ceti). I. Variable features of AlO and other Al-bearing species", *Astron. Astrophys.* **592** (2016), article no. A42.

[28] N. Fabas, A. Lèbre, D. Gillet, "Shock-induced polarized hydrogen emission lines in the Mira star *o* Ceti", *Astron. Astrophys.* **535** (2011), article no. A12.

[29] W. H. T. Vlemmings, T. Khouri, E. O'Gorman *et al.*, "The shock-heated atmosphere of an asymptotic giant branch star resolved by ALMA", *Nat. Astron.* **1** (2017), p. 848-853.

[30] W. Homan, E. Cannon, M. Montargès *et al.*, "A detailed view on the circumstellar environment of the M-type AGB star EP Aquarii. I. High-resolution ALMA and SPHERE observations", *Astron. Astrophys.* **642** (2020), article no. A93.

[31] P. Kervella, M. Montargès, E. Lagadec *et al.*, "The dust disk and companion of the nearby AGB star L_2 Puppis. SPHERE/ZIMPOL polarimetric imaging at visible wavelengths", *Astron. Astrophys.* **578** (2015), article no. A77.

[32] T. Khouri, W. H. T. Vlemmings, H. Olofsson *et al.*, "High-resolution observations of gas and dust around Mira using ALMA and SPHERE/ZIMPOL", *Astron. Astrophys.* **620** (2018), article no. A75.

[33] K. Ohnaka, G. Weigelt, K. H. Hofmann, "Clumpy dust clouds and extended atmosphere of the AGB star W Hydrae revealed with VLT/SPHERE-ZIMPOL and VLTI/AMBER. II. Time variations between pre-maximum and minimum light", *Astron. Astrophys.* **597** (2017), article no. A20.

[34] T. Khouri, W. H. T. Vlemmings, C. Paladini *et al.*, "Inner dusty envelope of the AGB stars W Hydrae, SW Virginis, and R Crateris using SPHERE/ZIMPOL", *Astron. Astrophys.* **635** (2020), article no. A200.

[35] T. Khouri, M. Maercker, L. B. F. M. Waters *et al.*, "Study of the inner dust envelope and stellar photosphere of the AGB star R Doradus using SPHERE/ZIMPOL", *Astron. Astrophys.* **591** (2016), article no. A70.

[36] B. R. M. Norris, P. G. Tuthill, M. J. Ireland *et al.*, "A close halo of large transparent grains around extreme red giant stars", *Nature* **484** (2012), p. 220-222.

[37] M. Hadjara, P. Cruzalebes, C. Nitschelm *et al.*, "A CO-multilayer outer atmosphere for eight evolved stars revealed with VLTI/AMBER", *Mon. Not. R. Astron. Soc.* **489** (2019), p. 2595-2614.

[38] R. Zhao-Geisler, R. Koehler, F. Kemper *et al.*, "Spectro-imaging of the asymmetric inner molecular and dust shell region of the mira variable W Hya with MIDI/VLTI", *Publ. Astron. Soc. Pac.* **127** (2015), p. 732-741.

[39] K. Ohnaka, G. Weigelt, K.-H. Hofmann, "Infrared interferometric three-dimensional diagnosis of the atmospheric dynamics of the AGB star R Dor with VLTI/AMBER", *Astrophys. J.* **883** (2019), article no. 89.

[40] D. Fedele, M. Wittkowski, F. Paresce *et al.*, "The K-band intensity profile of R Leonis probed by VLTI/VINCI", *Astron. Astrophys.* **431** (2005), p. 1019-1026.

[41] C. Paladini, D. Klotz, S. Sacuto *et al.*, "The VLTI/MIDI view on the inner mass loss of evolved stars from the Herschel MESS sample", *Astron. Astrophys.* **600** (2017), article no. A136.

[42] T. R. Bedding, A. A. Zijlstra, A. Jones *et al.*, "The light curve of the semiregular variable L_2 Puppis - I. A recent dimming event from dust", *Mon. Not. R. Astron. Soc.* **337** (2002), p. 79-86.

[43] T. R. Bedding, L. L. Kiss, H. Kjeldsen *et al.*, "The light curve of the semiregular variable L_2 Puppis - II. Evidence for solar-like excitation of the oscillations", *Mon. Not. R. Astron. Soc.* **361** (2005), p. 1375-1381.

[44] G. C. McIntosh, B. Indermühle, "The velocity centroid periodicity of L_2 Puppis' SiO maser emission", *Astrophys. J.* **774** (2013), article no. 21.

[45] P. Kervella, M. Montargès, S. T. Ridgway *et al.*, "An edge-on translucent dust disk around the nearest AGB star, L_2 Puppis. VLT/NACO spectro-imaging from 1.04 to 4.05 μm and VLTI interferometer", *Astron. Astrophys.* **564** (2014), article no. A88.

[46] F. Lykou, D. Klotz, C. Paladini *et al.*, "Dissecting the AGB star L_2 Puppis: a torus in the making", *Astron. Astrophys.* **576** (2015), article no. A46, erratum *Astron. Astrophys.* **581**, article no. C2.

[47] K. Ohnaka, D. Schertl, K. H. Hofmann, G. Weigelt, "AMBER-NACO aperture-synthesis imaging of the half-obscured central star and the edge-on disk of the red giant L_2 Puppis", *Astron. Astrophys.* **581** (2015), article no. A127.

[48] T. Khouri, L. Velilla-Prieto, E. De Beck *et al.*, "Detection of highly excited OH towards AGB stars. A new probe of shocked gas in the extended atmospheres", *Astron. Astrophys.* **623** (2019), article no. L1.

[49] D. T. Hoai, P. T. Nhung, P. Darriulat *et al.*, "Morpho-kinematics of the wind of asymptotic giant branch star L_2 Pup", *Mon. Not. R. Astron. Soc.* **510** (2022), p. 2363-2378.

[50] D. T. Hoai, P. T. Nhung, P. Darriulat *et al.*, "Recent mass ejection from AGB star W Hya", *VJSTE* **64** (2022), p. 16-27.

[51] D. T. Hoai, P. T. Nhung, M. N. Tan *et al.*, "Evidence for episodic and patchy mass ejection in the circumstellar envelope of AGB star R Leonis", *Mon. Not. R. Astron. Soc.* **518** (2023), p. 2034-2049.

[52] P. T. Nhung, D. T. Hoai, P. Tuan-Anh *et al.*, "Morpho-kinematics of the circumstellar envelope of the AGB star R Dor: a global view", *Mon. Not. R. Astron. Soc.* **504** (2021), p. 2687-2706.

[53] P. T. Nhung, D. T. Hoai, P. Darriulat *et al.*, "EP Aquarii: a new picture of the circumstellar envelope", *Res. Astrophys. Astron.* **24** (2024), article no. 035009.

[54] P. T. Nhung, D. T. Hoai, P. Tuan-Anh *et al.*, "Mira ceti, atypical archetype", *Astrophys. J.* **927** (2022), p. 169-184.

[55] D. T. Hoai, P. Tuan-Anh, P. T. Nhung *et al.*, "Revealing new features of the millimetre emission of the circumbinary envelope of Mira Ceti", *Mon. Not. R. Astron. Soc.* **495** (2020), p. 943-961.

[56] M. Karovska, E. Schlegel, H. Warren *et al.*, "A large X-ray outburst in Mira A", *Astrophys. J.* **623** (2005), p. 137-140.

[57] P. T. Nhung, D. T. Hoai, P. Tuan-Anh *et al.*, "The nascent wind of AGB star R doradus: evidence for a recent episode of enhanced mass loss", *Mon. Not. R. Astron. Soc.* **490** (2019), p. 3329-3340.

[58] E. De Beck, H. Olofsson, "Circumstellar environment of the M-type AGB star R Doradus. APEX spectral scan at 159.0–368.5 GHz", *Astron. Astrophys.* **615** (2018), article no. A8.

[59] W. Homan, T. Danilovich, L. Decin *et al.*, "ALMA detection of a tentative nearly edge-on rotating disk around the nearby AGB star R Doradus", *Astron. Astrophys.* **614** (2018), article no. A113.

[60] W. H. T. Vlemmings, T. Khouri, E. De Beck *et al.*, "Rotation of the asymptotic giant branch star R Doradus", *Astron. Astrophys.* **613** (2018), article no. L4.

[61] W. Homan, A. Richards, L. Decin *et al.*, "ALMA observations of the nearby AGB star L_2 Puppis. II. Gas disk properties derived from ^{12}CO and ^{13}CO $J = 3 - 2$ emission", *Astron. Astrophys.* **601** (2017), article no. A5.

[62] W. Homan, A. Richards, L. Decin *et al.*, "An unusual face-on spiral in the wind of the M-type AGB star EP Aquarii", *Astron. Astrophys.* **616** (2018), article no. A34.

[63] D. T. Hoai, P. T. Nhung, P. Tuan-Anh *et al.*, "Observation of high doppler velocity wings in the nascent wind of R Doradus", *Com. Phys. Vietnam* **30** (2020), p. 85-98.

[64] D. T. Hoai, P. T. Nhung, P. Tuan-Anh *et al.*, "The morpho-kinematics of the circumstellar envelope around the AGB star EP Aqr", *Mon. Not. R. Astron. Soc.* **484** (2019), p. 1865-1888.

[65] J.-M. Winters, T. Le Bertre, L.-A. Nyman *et al.*, "The hydrodynamical structure of circumstellar envelopes around low mass-loss rate, low outflow velocity AGB stars", *Astron. Astrophys.* **388** (2002), p. 609-614.

[66] P. Tuan-Anh, D. T. Hoai, P. T. Nhung *et al.*, "Observation of narrow polar jets in the nascent wind of oxygen-rich AGB star EP Aqr", *Mon. Not. R. Astron. Soc.* **487** (2019), p. 622-639.

[67] P. T. Nhung, D. T. Hoai, P. Darriulat *et al.*, "Contributions of rotation, expansion and line broadening to the morphology and kinematics of the inner CSE of oxygen-rich AGB star R Hya", *Res. Astrophys. Astron.* **23** (2023), article no. 015004.

[68] W. D. Cotton, B. Mennesson, P. J. Diamond *et al.*, "VLBA observations of SiO masers towards Mira variable stars", *Astron. Astrophys.* **414** (2004), p. 275-288.

[69] W. D. Cotton, W. H. T. Vlemmings, B. Mennesson *et al.*, "Further VLBA observations of SiO masers toward Mira variable stars", *Astron. Astrophys.* **456** (2006), p. 339-350.

[70] J. P. Fonfría, M. Santander-García, J. Cernicharo *et al.*, "Gas infall and possible circumstellar rotation in R Leonis", *Astron. Astrophys.* **622** (2019), article no. L14.

[71] G. Privitera, G. Meynet, P. Eggenberger *et al.*, "Star-planet interactions. II. Is planet engulfment the origin of fast rotating red giants?", *Astron. Astrophys.* **593** (2016), article no. A128.

[72] M. Morris, R. Sahai, K. Matthews *et al.*, "A binary-induced pinwheel outflow from the extreme carbon star, AFGL 3068", in *Planetary Nebulae in our Galaxy and Beyond, Proceedings IAU Symposium* (M. J. Barlow, R. H. Méndez, eds.), vol. 234, International Astronomical Union, Cambridge University Press, 2006, p. 469-470.

[73] S. K. Randall, A. Trejo, E. M. L. Humphreys *et al.*, "Discovery of a complex spiral-shell structure around the oxygen-rich AGB star GX Monocerotis", *Astron. Astrophys.* **636** (2020), article no. A123.

[74] S. Ramstedt, S. Mohamed, W. H. T. Vlemmings *et al.*, "The wonderful complexity of the Mira AB system", *Astron. Astrophys.* **570** (2014), article no. L14.

[75] H. M. Schmid, A. Bazzon, J. Milli *et al.*, "SPHERE/ZIMPOL observations of the symbiotic system R Aquarii. I. Imaging of the stellar binary and the innermost jet clouds", *Astron. Astrophys.* **602** (2017), article no. A53.

[76] V. Bujarrabal, J. Alcolea, J. Mikołajewska *et al.*, "High-resolution observations of the symbiotic system R Aqr. Direct imaging of the gravitational effects of the secondary on the stellar wind", *Astron. Astrophys.* **616** (2018), article no. L3.

[77] V. Bujarrabal, M. Agúndez, M. Gómez-Garrido *et al.*, "Structure and dynamics of the inner nebula around the symbiotic stellar system R Aquarii", *Astron. Astrophys.* **651** (2021), article no. A4.

[78] W. Homan, M. Montargès, B. Pimpanuwat *et al.*, "ATOMIUM: A high-resolution view on the highly asymmetric wind of the AGB star π1 Gruis. I. First detection of a new companion and its effect on the inner wind", *Astron. Astrophys.* **644** (2020), article no. A61.

[79] M. Schwarzschild, "On the scale of photospheric convection in red giants and supergiants", *Astrophys. J.* **195** (1975), p. 137-144.

[80] M. R. Templeton, M. Karovska, "Long-term variability in *o* Ceti and other Mira variables: Signs of supergranular convection?", in *Proceedings of the International Conference on Stellar Pulsation: Challenges for Theory and Observation*, AIP Conference Proceedings, vol. 1170, American Institute of Physics, Melville, NY, 2009, p. 164-166.

[81] M. R. Templeton, M. Karovska, "Long-Period Variability in *o* Ceti", *Astrophys. J.* **691** (2009), p. 1470-1478.

[82] L. L. Kiss, G. Szabó, T. R. Bedding, "Variability in red supergiant stars: pulsations, long secondary periods and convection noise", *Mon. Not. R. Astron. Soc.* **372** (2006), p. 1721-1734.

[83] M. Wittkowski, A. Chiavassa, B. Freytag *et al.*, "Near-infrared spectro-interferometry of Mira variables and comparisons to 1D dynamic model atmospheres and 3D convection simulations", *Astron. Astrophys.* **587** (2016), article no. A12.

[84] G. M. Vasil, K. Julien, N. A. Featherstone, "Rotation suppresses giant-scale solar convection", *Proc. Natl. Acad. Sci. USA* **118** (2021), article no. e2022518118.

[85] W. H. T. Vlemmings, "Magnetic fields of AGB and post-AGB stars", *Proc. IAUS* **343** (2019), p. 19-26.

[86] R. Montez Jr., S. Ramstedt, J. H. Kastner *et al.*, "A Catalog of GALEX ultraviolet emission from asymptotic giant branch stars", *Astrophys. J.* **841** (2017), article no. 33.

[87] E. G. Blackman, A. Frank, J. A. Markiel *et al.*, "Dynamos in asymptotic-giant-branch stars as the origin of magnetic fields shaping planetary nebulae", *Nature* **409** (2001), p. 485-487.

[88] G. Pascoli, L. Lahoche, "A magnetohydrodynamic model for the AGB star: preplanetary nebula symbiosis", *Publ. Astron. Soc. Pac.* **122** (2010), p. 1334-1340.

[89] A. Thirumalai, J. S. Heyl, "Is Mira a magneto-dusty rotator?", *Mon. Not. R. Astron. Soc.* **430** (2013), p. 1359-1368.

[90] A. Lèbre, M. Aurière, N. Fabas *et al.*, "Search for surface magnetic fields in Mira stars. First detection in χ Cygni", *Astron. Astrophys.* **561** (2014), article no. A85.

[91] A. Lèbre, M. Aurière, N. Fabas *et al.*, "Full Stokes IQUV spectropolarimetry of AGB and post-AGB stars: probing surface magnetism and atmospheric dynamics", *Proc. of the IAU* **305** (2015), p. 47-52.

[92] W. D. Cotton, G. Perrin, B. Lopez, "VLBA SiO observations of bright O-rich AGB stars", *Astron. Astrophys.* **477** (2008), p. 853-863.

[93] F. Herpin, A. Baudry, C. Thum *et al.*, "Full polarization study of SiO masers at 86 GHz", *Astron. Astrophys.* **450** (2006), p. 667-680.

[94] K. Y. Huang, A. J. Kemball, W. H. T. Vlemmings *et al.*, "Mapping circumstellar magnetic fields of late-type evolved stars with the Goldreich-Kylafis effect: CARMA observations at λ1.3 mm of R Crt and R Leo", *Astrophys. J.* **899** (2020), article no. 152.

[95] S. Uttenthaler, "Period-mass-loss rate relation of Miras with and without technetium", *Astron. Astrophys.* **556** (2013), article no. A38.

[96] S. Uttenthaler, I. McDonald, K. Bernhard *et al.*, "Interplay between pulsation, mass loss, and third dredge-up: More about Miras with and without technetium", *Astron. Astrophys.* **622** (2019), article no. A120.

[97] P. Merchan-Benitez, S. Uttenthaler, M. Jurado-Vargas, "Meandering periods and asymmetries in light curves of Miras: Observational evidence for low mass-loss rates?", *Astron. Astrophys.* **672** (2023), article no. A165.

[98] I. Cherchneff, "A chemical study of the inner winds of asymptotic giant branch stars", *Astron. Astrophys.* **456** (2006), p. 1001-1012.

[99] D. Duari, J. Hatchell, "HCN in the inner envelope of chi Cygni", *Astron. Astrophys.* **358** (2000), article no. L25.

[100] P. Marigo, E. Ripamonti, A. Nanni *et al.*, "Connecting the evolution of thermally pulsing asymptotic giant branch stars to the chemistry in their circumstellar envelopes—I. Hydrogen cyanide", *Mon. Not. R. Astron. Soc.* **456** (2016), p. 23-46.

[101] K. H. Hinkle, D. N. B. Hall, S. T. Ridgway, "Time series infrared spectroscopy of the Mira variable χ Cygni", *Astrophys. J.* **252** (1982), p. 697-714.

[102] F. Van Leeuwen, *Hipparcos, the New Reduction of the RawData*, Astrophysics and Space Science Library, vol. 350, Springer, Dordrecht, 2007.

[103] G. R. Knapp, D. Pourbaix, I. Platais *et al.*, "Reprocessing the Hipparcos data of evolved stars. III. Revised Hipparcos period-luminosity relationship for galactic long-period variable stars", *Astron. Astrophys.* **403** (2003), p. 993-1002.

[104] Gaia Collaboration, *VizieR Online Data Catalog*, vol. I/345, 2018.

[105] T. Dumm, H. Schild, "Stellar radii of M giants", *New Astron.* **3** (1998), p. 137-156.

[106] N. N. Samus, *VizieR Online Data Catalog: II/250*, 2004.

[107] C. L. Watson, "The international variable star index (VSX)", *JAAVSO* **35** (2006), p. 318.

[108] T. R. Bedding, A. A. Zijlstra, A. Jones *et al.*, "Mode switching in the nearby Mira-like variable R Doradus", *Mon. Not. R. Astron. Soc.* **301** (1998), p. 1073-1082.

[109] V. Tabur, T. R. Bedding, L. L. Kiss *et al.*, "Long-term photometry and periods for 261 nearby pulsating M giants", *Mon. Not. R. Astron. Soc.* **400** (2009), p. 1945-1961.

[110] O. J. Eggen, "Some small amplitude red variables of the disk and halo population", *Mem. R. Astr. Soc.* **77** (1973), p. 159.

[111] P. Planesas, J. Alcolea, R. Bachiller, "The radio continuum spectrum of Mira A and Mira B up to submillimeter wavelengths", *Astron. Astrophys.* **586** (2016), article no. A69.

[112] T. Danilovich, R. Lombaert, L. Decin *et al.*, "Water isotopologues in the circumstellar envelopes of M-type AGB stars", *Astron. Astrophys.* **602** (2017), article no. A14.

[113] T. Khouri, A. de Koter, L. Decin *et al.*, "The wind of W Hydrae as seen by Herschel. I. The CO envelope", *Astron. Astrophys.* **561** (2014), article no. A5.

[114] T. Khouri, A. de Koter, L. Decin *et al.*, "The wind of W Hydrae as seen by Herschel. II. The molecular envelope of W Hydrae", *Astron. Astrophys.* **570** (2014), article no. A67.

[115] H. W. Wiesemeyer, C. Thum, A. Baudry, F. Herpin, "Precessing planetary magnetospheres in SiO stars?. First detection of quasi-periodic polarization fluctuations in R Leonis and V Camelopardalis", *Astron. Astrophys.* **498** (2009), p. 801-810.

[116] N. Ryde, F. L. Schöier, "Modeling CO emission from Mira's wind", *Astrophys. J.* **547** (2001), p. 384-392.

[117] T. Danilovich, D. Teyssier, K. Justtanont *et al.*, "New observations and models of circumstellar CO line emission of AGB stars in the Herschel SUCCESS programme", *Astron. Astrophys.* **581** (2015), article no. A60.

[118] R. Zhao-Geisler, A. Quirrenbach, R. Köhler *et al.*, "Dust and molecular shells in asymptotic giant branch stars", *Astron. Astrophys.* **545** (2012), article no. A56.

[119] H. C. Woodruff, P. G. Tuthill, J. D. Monnier *et al.*, "The keck aperture masking experiment: multiwavelength observations of six mira variable", *Astrophys. J.* **673** (2008), p. 418-433.

[120] H. C. Woodruff, M. J. Ireland, P. G. Tuthill *et al.*, "The keck aperture masking experiment: spectro-interferometry of three mira variables from 1.1 to 3.8 μm".

[121] K. Tatebe, E. H. Wishnow, C. S. Ryan *et al.*, "The evolving shapes of *o* Ceti and R Leonis", *Astrophys. J.* **689** (2008), p. 1289-1294.

[122] T. Khouri, L. B. F. M. Waters, A. de Koter *et al.*, "Dusty wind of W Hydrae. Multi-wavelength modelling of the present-day and recent mass loss", *Astron. Astrophys.* **577** (2015), article no. A114.

[123] G. Perrin, V. Coudé du Foresto, S. T. Ridgway *et al.*, "Interferometric observations of R Leonis in the K band. First direct detection of the photospheric pulsation and study of the atmospheric intensity distribution", *Astron. Astrophys.* **345** (1999), p. 221-232.

[124] K.-H. Hofmann, Y. Balega, M. Scholz *et al.*, "Multi-wavelength bispectrum speckle interferometry of R Leo and comparison with Mira star models", *Astron. Astrophys.* **376** (2001), p. 518-531.

[125] T. Kamínski, H. S. P. Müller, M. R. Schmidt *et al.*, "An observational study of dust nucleation in Mira (*o* Ceti). II. Titanium oxides are negligible for nucleation at high temperatures", *Astron. Astrophys.* **599** (2017), article no. A59.

[126] T. Danilovich, M. Van de Sande, E. De Beck *et al.*, "Sulphur-bearing molecules in AGB stars. I. The occurrence of hydrogen sulphide", *Astron. Astrophys.* **606** (2017), article no. A124.

[127] T. Danilovich, E. De Beck, J. H. Black *et al.*, "Sulphur molecules in the circumstellar envelopes of M-type AGB stars", *Astron. Astrophys.* **588** (2016), article no. A119.

[128] P. T. Nhung, D. T. Hoai, P. N. Diep *et al.*, "Morphology and kinematics of the gas envelope of Mira Ceti", *Mon. Not. R. Astron. Soc.* **460** (2016), p. 673-688.

[129] T. Khouri, W. H. T. Vlemmings, S. Ramstedt *et al.*, "ALMA observations of the vibrationally excited rotational CO transition $v = 1$, $J = 3 - 2$ towards five AGB stars", *Mon. Not. R. Astron. Soc.* **463** (2016), article no. L74.

[130] D. T. Hoai, P. Tuan-Anh, P. T. Nhung *et al.*, "ALMA observations of W Hya: impact of missing baselines", *JKAS* **54** (2021), p. 171-182.

[131] J. P. Fonfría, "Poster Presented at the ALMA2019: Science Results and Cross-facility Synergies, Cagliari", 2019.

[132] M. J. Reid, K. M. Menten, "Imaging the radio photospheres of mira variables", *Astrophys. J.* **671** (2007), p. 2068-2073.

[133] L. D. Matthews, M. J. Reid, K. M. Menten *et al.*, "The evolving radio photospheres of long-period variable stars", *Astron. J.* **156** (2018), article no. 15.

[134] J. R. Rizzo, J. Cernicharo, C. Garciá-Míro, "SiO, ^{29}SiO, and ^{30}SiO emission from 67 oxygen-rich stars: a survey of 61 maser lines from 7 to 1 mm", *ApJS* **253** (2021), article no. 44.

[135] W. H. T. Vlemmings, T. Khouri, D. Tafoya, "Maser emission from the CO envelope of the asymptotic giant branch star W Hydrae", *Astron. Astrophys.* **654** (2021), article no. A18.

[136] W. D. Cotton, S. Ragland, E. Pluzhnik *et al.*, "SIO masers in asymmetric miras. I. R Leonis", *Astrophys. J.* **704** (2009), p. 170-182.

[137] R. Soria-Ruiz, J. Alcolea, F. Colomer *et al.*, "Mapping the circumstellar SiO maser emission in R Leonis", *Astron. Astrophys.* **468** (2007), article no. L1.

[138] J.-F. Desmurs, V. Bujarrabal, M. Lindqvist *et al.*, "SiO masers from AGB stars in the vibrationally excited $v = 1$, $v = 2$, and $v = 3$ states", *Astron. Astrophys.* **565** (2014), article no. A127.

[139] M. Wenger, F. Ochsenbein, D. Egret *et al.*, "The SIMBAD astronomical database. The CDS reference database for astronomical objects", *Astron. Astrophys.* **143** (2000), p. 9-22.

[140] N. N. Samus, *VizieR Online Data Catalog: B/GCVS*, 2009.

[141] A. G. A. Gaia Collaboration, Brown, A. Vallenari *et al.*, *Astron. Astrophys.* **649** (2021), article no. A1.

[142] H. van Langevelde, L. H. Quiroga-Nunez, W. Vlemmings *et al.*, "The Synergy between VLBI and Gaia astrometry", in *Proceedings of the 14th European VLBI Network Symposium & Users Meeting, Granada*, vol. 344, EVN publications, 2019.